

Assessing the near surface sensitivity of SCIAMACHY atmospheric CO₂ retrieved using (FSI) WFM-DOAS

M. P. Barkley^{1,*}, P. S. Monks², A. J. Hewitt¹, T. Machida³, A. Desai⁴,
N. Vinnichenko^{5,†}, T. Nakazawa⁶, M. Yu Arshinov⁷, N. Fedoseev⁸, and T. Watai⁹

¹EOS, Department of Physics and Astronomy, University of Leicester, UK

²Department of Chemistry, University of Leicester, UK

³National Institute for Environmental Studies, Tsukuba, Japan

⁴National Centre for Atmospheric Research, Boulder, Colorado, USA

⁵Central Aerological Observatory, Dolgoprudny, Russia

⁶Tohoku University, Sendai, Japan

⁷Institute of Atmospheric Optics, Tomsk, Russia

⁸Permafrost Institute, Yakutsk, Russia

⁹Global Environmental Forum, Tsukuba, Japan

* now at: Institute for Atmospheric and Environmental Science, School of GeoSciences,
University of Edinburgh, UK

†deceased 2006

Received: 30 January 2007 – Accepted: 15 February 2007 – Published: 21 February 2007

Correspondence to: P. S. Monks (psm7@le.ac.uk)

SCIAMACHY
atmospheric CO₂

Barkley et al.

Title Page

Abstract

Introduction

Conclusions

References

Tables

Figures

◀

▶

◀

▶

Back

Close

Full Screen / Esc

Printer-friendly Version

Interactive Discussion

EGU

Abstract

Satellite observations of atmospheric CO₂ offer the potential to identify regional carbon surface sources and sinks and to investigate carbon cycle processes. The extent to which satellite measurements are useful however, depends on the near surface sensitivity of the chosen sensor. In this paper, the capability of the SCIAMACHY instrument on board ENVISAT, to observe lower tropospheric and surface CO₂ variability is examined. To achieve this, atmospheric CO₂ retrieved from SCIAMACHY near infrared (NIR) spectral measurements, using the Full Spectral Initiation (FSI) WFM-DOAS algorithm, is compared to in situ aircraft observations over Siberia and additionally to tower and surface CO₂ data over Mongolia, Europe and North America.

Preliminary validation of daily averaged SCIAMACHY/FSI CO₂ against ground based Fourier Transform Spectrometer (FTS) column measurements made at Park Falls, reveal a negative bias of about -2.0% for collocated measurements within ±1.0° of the site. However, at this spatial threshold SCIAMACHY can only capture the variability of the FTS observations at monthly timescales. To observe day to day variability of the FTS observations, the collocation limits must be increased. Furthermore, comparisons to in-situ CO₂ observations demonstrate that SCIAMACHY is capable of observing lower tropospheric variability on (at least) monthly timescales. Out of seventeen time series comparisons, eleven have correlation coefficients of 0.7 or more, and have similar seasonal cycle amplitudes. Additional evidence of the near surface sensitivity of SCIAMACHY, is provided through the significant correlation of FSI derived CO₂ with MODIS vegetation indices at over twenty selected locations in the United States. The SCIAMACHY/MODIS comparison reveals that at many of the sites, the amount of CO₂ variability is coincident with the amount of vegetation activity. It is evident, from this analysis, that SCIAMACHY therefore has the potential to detect CO₂ variability within the lowermost troposphere arising from the activity of the terrestrial biosphere.

ACPD

7, 2477–2530, 2007

SCIAMACHY atmospheric CO₂

Barkley et al.

Title Page

Abstract

Introduction

Conclusions

References

Tables

Figures

◀

▶

◀

▶

Back

Close

Full Screen / Esc

Printer-friendly Version

Interactive Discussion

EGU

1 Introduction

Although water vapour is by far the dominant greenhouse gas, contributing to 60% of the greenhouse effect, its short residence time (~ 10 days) means that it is considered as a natural feedback, rather than forcing agent (Kiehl and Trenberth, 1997). Of the anthropogenic greenhouse gases, carbon dioxide (CO_2) generates the largest forcing and is considered the principal species with methane (CH_4) the next most important. Whereas at any given instant the mean global energy balance is governed by water vapour and clouds, over long time scales (i.e. decades and longer) it is predominately regulated by CO_2 . Over the last 200 years there has been a dramatic $\sim 30\%$ rise in atmospheric CO_2 owing primarily to the burning of fossil fuels and deforestation. This significant increase is likely to have a serious impact on the carbon cycle and climate, as present concentrations are now greater than at any other time in the last half a million years (Siegenthaler et al., 2005).

Two important carbon cycle sinks which absorb CO_2 from the atmosphere, and keep levels lower than otherwise, are the terrestrial biosphere and the ocean. The terrestrial biosphere draws down CO_2 through the creation and accumulation of plant biomass, whereas CO_2 that diffuses across the atmosphere-ocean interface is mixed to deep waters by the solubility, biological and carbonates pumps. However, there is much uncertainty about where, and how, this uptake occurs. As global carbon emissions show no sign of slowing, the variability and efficiency of the terrestrial and oceanic sinks will play an important role in shaping the Earth's future climate. Present estimates of the global carbon cycle fluxes, provided by inverse modelling (e.g. Rödenbeck et al., 2003; Patra et al., 2006), are restricted by the sparse distribution and limited number of available measurements (Gurney et al., 2002). The greater spatial and temporal coverage offered by satellite observations, if of sufficient ($\sim 1\%$) precision, coupled with inverse models can help identify surface sources and sinks and reduce flux uncertainties (O'Brien and Rayner, 2002; Houweling et al., 2004). Satellite observations therefore offer an unique ability to investigate the dynamics of the carbon cycle. However,

Title Page

Abstract

Introduction

Conclusions

References

Tables

Figures

◀

▶

◀

▶

Back

Close

Full Screen / Esc

Printer-friendly Version

Interactive Discussion

one of the most important aspects of satellite CO₂ measurements is the question of near-surface sensitivity i.e. can the instrument observe CO₂ variability within the lower troposphere, where the signatures of surface fluxes occur?

Thermal infrared sounders, such as AIRS, have limited sensitivity to surface CO₂ as the light that the sensor detects originates from the mid-upper troposphere (Engelen and McNally, 2005; Tiwari et al., 2006). In contrast, NIR instruments such as SCIAMACHY (the only current operational NIR sensor) or the future OCO and GOSAT missions, are sensitive to the lower troposphere since they detect light that is reflected from the Earth's surface i.e. which has traversed the atmospheric path completely. Previous work by Buchwitz et al. (2005a,b, 2006), Houweling et al. (2005) and Barkley et al. (2006a,b,c) have shown that CO₂ measurements from SCIAMACHY are possible with a precision that is approaching the 1% threshold requirement.

In this paper, SCIAMACHY CO₂, retrieved using the (FSI) WFM-DOAS algorithm (Barkley et al., 2006a,b,c), is initially validated against ground based Fourier Transform Spectrometer (FTS) column measurements and then compared to in situ aircraft, tower and surface CO₂ observations to assess if SCIAMACHY is able to detect changes in surface CO₂ concentrations. Although SCIAMACHY measures the CO₂ column integral, in situ observations of atmospheric CO₂ mixing ratios made at the surface or from aircraft can provide a useful comparison data set. However, care must be taken when performing any analysis. In situ observations occur at a specific location, time and altitude whereas typically the SCIAMACHY CO₂ corresponds to a column VMR which is often given as a monthly gridded product (to improve the precision). Thus, a comparison of the magnitudes, phasing and the general behaviour of the seasonal cycle are often the only features that can be examined with any meaning. Thus, validation of SCIAMACHY CO₂ using surface data will, for the most part, be performed using monthly average time series although comparisons to spatially and temporally collocated aircraft measurements over Siberia are demonstrated.

Furthermore, in the second part of this paper, the North American region is selected for a case study. The spatial distributions over this scene for 2003 and 2004 are ex-

**SCIAMACHY
atmospheric CO₂**

Barkley et al.

Title Page

Abstract

Introduction

Conclusions

References

Tables

Figures

◀

▶

◀

▶

Back

Close

Full Screen / Esc

Printer-friendly Version

Interactive Discussion

5 amined whilst additionally vegetation proxy data, taken from the MODIS instrument, is compared to SCIAMACHY CO₂ at over twenty locations within the US to assess if there is any observable correlation between terrestrial vegetation activity and atmospheric CO₂ concentrations. Any significant correlation between SCIAMACHY derived

10 CO₂ and vegetation at specific locations will be further evidence of near surface sensitivity. This paper is structured as follows. Section 2 contains a brief description of SCIAMACHY whilst Sect. 3 gives an overview of the FSI retrieval algorithm. Validation of SCIAMACHY/FSI CO₂ against ground based FTS measurements is discussed in Sect. 4 with the detailed comparisons to aircraft, tower and surface measurements performed in Sect. 5. The case study over North America is documented in Sect. 6 with overall conclusions given in Sect. 7.

2 The SCIAMACHY instrument

15 The SCanning Imaging Absorption spectrometer for Atmospheric CHartography (SCIAMACHY) instrument is a passive UV-VIS-NIR hyper-spectral spectrometer designed to investigate atmospheric composition and processes (Bovensmann et al., 1999; Gottwald et al., 2006). It was launched onboard the ENVISAT satellite, in March 2002, into a near polar sun-synchronous orbit, from which it can observe the Earth from three viewing geometries: nadir, limb and lunar/solar occultation. The instrument

20 measures sunlight that is reflected from the surface or scattered by the atmosphere, covering the spectral range 240–2380 nm (non-continuously) using eight separate grating spectrometers (or channels), with moderate spectral resolution 0.2–1.4 nm. For the majority of its orbit SCIAMACHY make measurements in an alternating limb and nadir sequence. The total columns of CO₂ are derived from nadir observations in the NIR, using a small micro-window within channel six, centered on the CO₂ band at 1.57 μm.

25 For channel 6, the nominal size of each pixel within the 960×30 km² (across×along track) swath is 60×30 km² which corresponds to an integration time of 0.25 s. Global

Title Page

Abstract

Introduction

Conclusions

References

Tables

Figures

◀

▶

◀

▶

Back

Close

Full Screen / Esc

Printer-friendly Version

Interactive Discussion

coverage is achieved at the Equator within 6 days.

3 Full Spectral Initiation (FSI) WFM-DOAS

The Full Spectral Initiation (FSI) WFM-DOAS retrieval algorithm, discussed in detail in [Barkley et al. \(2006a,b,c\)](#), has been developed specifically to retrieve CO₂ from space using SCIAMACHY NIR spectral measurements. It is a development of the WFM-DOAS algorithm first introduced by [Buchwitz et al. \(2000\)](#) whereby the trace gas vertical column density (VCD) can be retrieved through a linear least squares fit of the logarithm of a model reference spectrum I_i^{ref} and its derivatives, plus a quadratic polynomial P_i , to the logarithm of the measured sun normalized intensity I_i^{meas} :

$$\left\| \ln I_i^{\text{meas}}(\mathbf{V}^t) - \left[\ln I_i^{\text{ref}}(\bar{\mathbf{V}}) + \sum_j \frac{\partial \ln I_i^{\text{ref}}}{\partial \bar{V}_j} \cdot (\hat{V}_j - \bar{V}_j) + P_i(a_m) \right] \right\|^2 \equiv \|\text{RES}_i\|^2 \rightarrow \min \text{ w.r.t } \hat{V}_j \text{ \& } a_m \quad (1)$$

where the subscript i refers to each detector pixel of centre wavelength λ_i and the true, model and retrieved vertical columns are represented by $\mathbf{V}^t = (V_{\text{CO}_2}^t, V_{\text{H}_2\text{O}}^t, V_{\text{Temp}}^t)$, $\bar{\mathbf{V}} = (\bar{V}_{\text{CO}_2}, \bar{V}_{\text{H}_2\text{O}}, \bar{V}_{\text{Temp}})$ and \hat{V}_j respectively (where j refers to the variables CO₂, H₂O and temperature). Each derivative represents the change in radiance at the top of the atmosphere as a function of a relative scaling of the corresponding trace gas or temperature profile. It should be noted that V_{Temp} is not a vertical column but rather a scaling factor applied to the vertical temperature profile. The fit parameters are the trace gas columns \hat{V}_{CO_2} and $\hat{V}_{\text{H}_2\text{O}}$, the temperature scaling factor \hat{V}_{Temp} and the polynomial coefficients a_m . The error, associated with each of the fit parameters, is given by Eq. (2) where $(\mathbf{C}_\mathbf{x})_{jj}$ refers to the j th diagonal element from the least squares fit covariance matrix, RES_i is

Title Page

Abstract

Introduction

Conclusions

References

Tables

Figures

◀

▶

◀

▶

Back

Close

Full Screen / Esc

Printer-friendly Version

Interactive Discussion

the fit residual, m is the number of spectral points within the fitting window and n is the number of fit parameters.

$$\sigma_{\hat{V}_j} = \sqrt{\frac{(\mathbf{C}_x)_{jj} \times \sum_i RES_i^2}{(m - n)}} \quad (2)$$

The main focuss of the FSI algorithm is the inclusion of a priori data within the retrieval in order to minimize the error associated with the retrieved CO₂ column. The FSI algorithm differs from current implementations of WFM-DOAS (e.g. Buchwitz et al., 2005b, 2006) in that rather than using a look-up table approach, it generates a reference spectrum for each individual SCIAMACHY observation. Each model spectrum is created using the radiative transfer model SCIATRAN (Rozanov et al., 2002), which includes the latest version of the HITRAN molecular spectroscopic database (Rothman et al., 2005), from several sources of a priori data including:

- A CO₂ vertical profile is selected from a specially prepared climatology (Remedios et al., 2006)
- Temperature, pressure and water vapour profiles, derived from operational 6 hourly ECMWF data (1.125° × 1.125° grid)
- An approximate value for the surface albedo is inferred using the mean radiance (within the fitting window) and the solar zenith angle of the SCIAMACHY observation
- Maritime, rural and urban aerosol scenarios are implemented over the oceans, land and urban areas respectively using the LOWTRAN aerosol model (Kneizys et al., 1996).

As the line by line calculation of radiances is computationally expensive, the FSI algorithm is not implemented on an iterative basis. Instead, each reference spectrum

Title Page

Abstract

Introduction

Conclusions

References

Tables

Figures

◀

▶

◀

▶

Back

Close

Full Screen / Esc

Printer-friendly Version

Interactive Discussion

[Title Page](#)[Abstract](#)[Introduction](#)[Conclusions](#)[References](#)[Tables](#)[Figures](#)[◀](#)[▶](#)[◀](#)[▶](#)[Back](#)[Close](#)[Full Screen / Esc](#)[Printer-friendly Version](#)[Interactive Discussion](#)

is only used as the best possible linearization point for the retrieval. The potential error from not performing any iterations is kept to a minimum, since the a priori data generate model spectra that closely approximate SCIAMACHY measurements. In order to avoid possible instrumental issues, that hinder retrievals when using the NIR channels (e.g. Gludemans et al., 2005), the raw SCIAMACHY spectra (v5.04) are calibrated in-house. Corrections for the orbit specific dark current and detector non-linearity (Kleipool, 2003a,b) are applied. Furthermore, a solar spectrum with improved calibration is also used (courtesy of ESA). All SCIAMACHY observations are cloud screened prior to retrieval processing, using the cloud detection method devised by Krijger et al. (2005), with cloud contaminated pixels flagged and disregarded. Back-scans along with observations that have solar zenith angles greater than 75° are also not processed. To produce a CO₂ vertical column volume mixing ratio (VMR) each retrieved VCD is normalized using the input ECMWF surface pressure. To clean the data from potential biases arising from aerosols or undetected (and partial) cloud contamination only VMRs that have retrieval errors less than 5% and that are within the range 340–400 ppmv are used. Any CO₂ column VMRs lying outside this range are classed as failed retrievals.

4 Validation of SCIAMACHY CO₂ using park falls FTS measurements

Measurements of the CO₂ column integral by ground based Fourier Transform Spectrometers (FTS) provide the most useful means of validating satellite CO₂ observations (e.g. Dils et al., 2006). Previous validation of SCIAMACHY/FSI CO₂ to FTS CO₂ measurements, made at Egbert (Canada) revealed a negative bias of about –4% to the true CO₂ concentration (Barkley et al., 2006c). However, the Egbert site is in the region of the large urban centre of Tronto and thus may suffer from local contamination. A more suitable location for satellite CO₂ validation is the Park Falls site located within northern Wisconsin, where existing surface and tower CO₂ measurements are already made (e.g. Bakwin and Tans, 1995). The FTS based at this site, which is part of the

Title Page

Abstract

Introduction

Conclusions

References

Tables

Figures

◀

▶

◀

▶

Back

Close

Full Screen / Esc

Printer-friendly Version

Interactive Discussion

EGU

Total Carbon Column Observing Network (TCCON)¹, has already been used to test the OCO retrieval algorithm using SCIAMACHY NIR measurements (Bösch et al., 2006). The site itself, is surrounded by boreal and wetland forests and relatively flat terrain.

In this paper, measurements of the CO₂ column made by Washenfelder et al. (2006) are used to further assess the accuracy of the FSI retrieved CO₂. As the FTS measurement procedure is thoroughly documented in Washenfelder et al. (2006) a brief outline of the experimental set-up is only given here. The CO₂ columns are derived from solar absorption spectra recorded by a Bruker 125HR FTS housed within a steel shipping container, adjacent to the WLEF TV tower that is situated at the site. The FTS is fully automated with an active solar tracker directing light, from the centre of the solar disk, into the FTS instrument which has a 2.4 mrad field of view. Dual detectors InGasAs and Si-diode detectors then simultaneously record solar spectra over the interval 3800–15 500 cm⁻¹ at high resolution (0.014 cm⁻¹) which is sufficient to resolve individual CO₂ lines. Simultaneous retrieval of the CO₂ column from two bands centred at 6228 cm⁻¹ and 6348 cm⁻¹ and of the O₂ column from the band at 7882 cm⁻¹ is achieved using the non-linear least squares spectral fitting (GFIT) algorithm developed at the Jet Propulsion Laboratory. The CO₂ dry column average is then calculated via CO₂/O₂ × 0.295. Under clear sky observations the measurement precision is 0.1%. Calibration against integrated aircraft profiles indicate a small bias of ~ -2.0% but good correlation.

To determine the accuracy of FSI retrieved CO₂, daily averaged SCIAMACHY observations, denoted *SCIA_D*, collocated within incremental longitude and latitude limits of the Park Falls site (see Table 1), were directly compared to the daily mean FTS CO₂ VMR, denoted *PF_D*, if available. The bias of each SCIAMACHY CO₂ column with respect to the ground based measurement is then given by:

$$\text{Bias} = \left(\frac{\text{SCIA}_D - \text{PF}_D}{\text{PF}_D} \right) \times 100\% \quad (3)$$

¹See www.tcon.caltech.edu.

with the mean bias B , then simply the average over all the SCIAMACHY/FTS match-ups. By applying the averaging kernels (Fig. 2) of SCIAMACHY and the FTS to the CO₂ climatology, it has been verified that differences in the CO₂ columns owing to the different sensitivities (i.e. averaging kernels) of each instrument are small: $\sim 1\text{--}2$ ppmv (see, e.g. Bösch et al., 2006).

As Table 1 shows, the bias to the FTS measurements is very dependent on the collocation boundary limits selected around the Park Falls site. At close proximity, i.e. within $0.5^\circ \times 0.5^\circ$, the mean bias is -3.1% however the number of SCIAMACHY/FTS match-ups N_c is small and few SCIAMACHY observations, indicated by N_{FSI} , are used to calculate the daily mean. At very large collocation limits (e.g. $10.0^\circ \times 10.0^\circ$) this bias is reduced to only -0.9% owing both to the greater number of match-ups and the greater number of SCIAMACHY observations used to calculate SCIA_D. The precision and accuracy of SCIAMACHY/FSI CO₂ is therefore significantly improved by the averaging process. This is reflected in the scatter of the SCIAMACHY data, which is reduced as N_{FSI} increases. The negative bias that is found for each of the collocation limits is better than, but consistent with, the -4.0% offset observed at Egbert (Barkley et al., 2006c).

For SCIAMACHY observations occurring within $1.0^\circ \times 1.0^\circ$ of Park Falls (which is the spatial resolution of monthly gridded FSI data) the bias is -2.1% but the correlation between the SCIAMACHY and FTS daily means is quite low at 0.36. This implies that SCIAMACHY fails to capture the day to day variability of the FTS measurements. Only once the collocation boundaries are expanded to at least $3.0^\circ \times 3.0^\circ$ (and above) does the correlation become significant. However, if the $1.0^\circ \times 1.0^\circ$ limits are again used but with both data sets assembled into monthly averages then the bias is -2.2% but the correlation improves to 0.94. This means that to capture day to day variability around Park Falls (or any FTS site) a wider overpass criteria must be tolerated but to capture monthly variability collocation limits of $1.0^\circ \times 1.0^\circ$ resolution are acceptable. Either way the bias is about -2.0% .

Title Page

Abstract

Introduction

Conclusions

References

Tables

Figures

◀

▶

◀

▶

Back

Close

Full Screen / Esc

Printer-friendly Version

Interactive Discussion

5 Assessing the near surface sensitivity of SCIAMACHY

5.1 Model simulations

The SCIAMACHY/FSI averaging kernels peak in the planetary boundary layer indicating increased sensitivity to the lower atmosphere (Fig. 2). However, before comparisons between SCIAMACHY and in situ surface data are made, it is necessary to use model simulations to ascertain what one would expect SCIAMACHY to observe as compared to the seasonal signal within the lower troposphere. To achieve this, simulated retrievals were performed using spectra generated from CO₂ profiles taken from the newly prepared climatology (Remedios et al., 2006). This climatology consists of 12 monthly profiles for each 30° latitude band (see, e.g. Fig. 1 of Barkley et al., 2006a). In each simulation, a “measurement” spectrum was created by inputting into SCIATRAN the climatological CO₂ profile (interpolated onto the US Standard pressure scale) along with the US Standard temperature and water vapour profile. Then, using a uniform a priori CO₂ profile scaled to 370 ppmv, a simulated retrieval performed with the retrieved (normalized) column VMR compared to the mixing ratio of the climatological CO₂ profile at the surface and also at selected altitudes between 0–5 km.

The results of these simulations reveal that below 30°N the difference between the retrieved column VMR and those at the surface are very similar. In terms of absolute magnitudes, the column VMRs below 30° N are larger than those mixing ratios at the surface. Furthermore, the magnitude of the seasonal cycles and their phasing of their anomalies (not shown), are almost indistinguishable. Between 60–90° N, the phasing between the surface and column VMRs also agrees well (Fig. 3). This is in spite of the fact the retrieved columns VMRs are lower in the spring months, relative to the mixing ratios at the surface and correspondingly higher in the summer months. Furthermore, within this latitude band, the seasonal cycle amplitude of the retrieved column VMRs (11.3 ppmv) is 2.3 ppmv higher than that of true column seasonal amplitude, whereas it is smaller when compared to the seasonal cycle observed at the surface, which it is typically ~14–15 ppmv. The mean amplitude over 0–5 km is however is marginally

Title Page

Abstract

Introduction

Conclusions

References

Tables

Figures

◀

▶

◀

▶

Back

Close

Full Screen / Esc

Printer-friendly Version

Interactive Discussion

larger than that of the retrieved column, 13.4 ppmv as compared to 11.3 ppmv.

The seasonal cycles between 30–60° N are similar to those at higher latitudes with the exception that the phasing of the retrieved column VMRs slightly lags behind that at the surface at the spring/summer crossover of the CO₂ anomaly (i.e. when photosynthesis exceeds respiration). The delay of the crossover is coherent with the transport and vertical mixing of the seasonal signal from the surface to higher altitudes. Within this latitude range, the retrieved column VMR seasonal amplitude is 1.5 ppmv lower than that over 0–5 km but approximately 1 ppmv greater than the true column signal.

Thus, if one assumes that monthly averaged surface data is adequately representative of well mixed CO₂ below 5 km then, at mid to high northern latitudes, SCIAMACHY should see a seasonal signal smaller than that at the surface but which is in turn larger than that of the true seasonal amplitude of the column integral. Moreover, the phasing at high northern latitudes is expected to be consistent with that at the surface whilst at mid-latitudes a slight shift is more likely. In the southern hemisphere, the seasonal cycles amplitudes of the column VMRs should be of the same order of those at the surface with approximately the same phasing.

5.2 Comparison to aircraft CO₂ over Siberia

In this section, SCIAMACHY CO₂ column VMRs are compared to volume mixing ratios (vmrs) measured from aircraft flights, made in 2003, over three Siberian locations: Novosibirsk, Surgut and Yakutsk (Fig. 4). The CO₂ volume mixing ratios were determined using the air-sampling method as outlined in Machida et al. (2001). Over Novosibirsk and Surgut, chartered AN-30 and AN-24 aircraft were used respectively with samples taken by pressurizing air, fed into the cockpit through a drain pipe, into a 0.5 L Pyrex glass flask using a diaphragm pump. These systems were operated manually with the aircraft sampling at eight different altitudes between 0.0–7.0 km over both of these sites. Over Yakutsk, a smaller AN-2 aircraft was used which only sampled the altitudes 0.0–3.0 km during 2003. The CO₂ volume mixing ratios were derived from the flask samples to an accuracy of ~0.10 ppmv, against standard gases, using a

Title Page

Abstract

Introduction

Conclusions

References

Tables

Figures

◀

▶

◀

▶

Back

Close

Full Screen / Esc

Printer-friendly Version

Interactive Discussion

non-dispersive infrared analyzer (NDIR) at either Tohoku University, Japan (for Surgut measurements) or the National Institute for Environmental Studies (NIES), Japan (for Novosibirsk and Yakutsk measurements). To capture discrete events, SCIAMACHY observations occurring on the same day of each flight and collocated within $\pm 10.0^\circ$ longitude and $\pm 8.0^\circ$ latitude of each location, were averaged and compared to the mean of the aircraft measurements (convolved with a mean SCIAMACHY averaging kernel) over all sampling altitudes.

Over Yakutsk, the agreement between the aircraft CO_2 vmrs and the column VMRs measured by SCIAMACHY is poor (e.g. Fig. 5). However, the aircraft observations agree with SCIAMACHY on the timing and approximate magnitude of the minimum CO_2 at the end of July. The average difference between SCIAMACHY CO_2 and the mean aircraft CO_2 (over all altitudes) is typically less than 4% with the smallest difference occurring in July. The CO_2 anomalies, that is each measurement minus the mean of its data set, show similar behaviour with the best agreement being between the middle of May to the beginning of July when a significant amount of CO_2 uptake occurs. That said, the minimum of the aircraft anomaly dips lower than that of SCIAMACHY though the size of the return, between July and October, is approximately the same (8.7 ppmv for SCIAMACHY and 10.7 ppmv for the aircraft observations). The amplitude of the seasonal signal observed by the aircraft varies considerably with altitude and has a mean of 25.0 ppmv which is noticeably larger than that detected by SCIAMACHY (17.5 ppmv). The correlation between SCIAMACHY and the mean of the aircraft data is 0.72.

Over Novosibirsk, the overall difference between the mean aircraft CO_2 and SCIAMACHY is smaller than at that found at Yakutsk, only approximately 2% or so (Fig. 6) with the correlation 0.77. The aircraft data show an extremely large seasonal cycle amplitude in the lowest 1 km of >40 ppmv which decreases with altitude. SCIAMACHY observes a smaller seasonal amplitude of 21.0 ppmv which is thus more comparable to the mean aircraft seasonal which is 23.5 ppmv. Examination of Fig. 7 reveals that in addition, the CO_2 anomalies measured over Novosibirsk show very good agreement

[Title Page](#)[Abstract](#)[Introduction](#)[Conclusions](#)[References](#)[Tables](#)[Figures](#)[I◀](#)[▶I](#)[◀](#)[▶](#)[Back](#)[Close](#)[Full Screen / Esc](#)[Printer-friendly Version](#)[Interactive Discussion](#)

between March–July. The change in the anomalies between October and December is also similar.

Over Surgut there were only six coincidental SCIAMACHY observations. Nevertheless, there is fairly good agreement between SCIAMACHY and the aircraft observations. The volume mixing ratios are of the same order of magnitude and the typical difference from mean aircraft observations is ~2%. Unlike the measurements over Yakutsk or Novosibirsk, the amplitude of the seasonal cycle detected by SCIAMACHY (26.0 ppmv) is larger than the aircraft observations at any altitude or over any altitude range. At the surface, the seasonal amplitude is 19.9 ppmv which decreases rapidly with altitude to only 8.3 ppmv at 7.0 km. Thus, even though a quite strong seasonal cycle is evident at the surface it doesn't propagate to higher altitudes.

In summary, the FSI retrieved CO₂ shows fair agreement to the aircraft observations. Whilst the precision of the raw satellite columns is less than that of the monthly gridded data, the variation of atmospheric CO₂ over the selected Siberian locations is still captured by SCIAMACHY if large collocation limits are used.

5.3 Comparison to in-situ surface observations

5.3.1 Europe and Mongolia

In addition to the aircraft comparison over Siberia, SCIAMACHY CO₂ has also been compared to ground based in-situ observations taken from the World Data Centre for Greenhouse Gases (WDCGG) network². In this section this comparison is confined to Western Europe and to Mongolia (since SCIAMACHY retrievals over these region have already been processed for the TM3 model comparison documented in Barkley et al., 2006c). Within western Europe there were only five sampling sites which had CO₂ data for 2003 (shown in Fig. 8) whilst in Mongolia there was only a single station at Ulan Uul (47° N, 111° E). The CO₂ volume mixing ratios are measured, on a con-

²Downloadable from <http://gaw.kishou.go.jp/wdogg.html>

Title Page

Abstract

Introduction

Conclusions

References

Tables

Figures

◀

▶

◀

▶

Back

Close

Full Screen / Esc

Printer-friendly Version

Interactive Discussion

tinuous or weekly basis, at these locations using NDIR analyzers. In this analysis, the monthly averages of the ground based observations have been used, since the ability of SCIAMACHY to detect seasonal variations is being assessed. For this reason, the selection criteria for collocated satellite observations was based on using monthly (1° × 1°) gridded SCIAMACHY data, with the average taken of all grid points lying within ±3.5° latitude and ±5.0° longitude of each site. These collocation limits were chosen as a compromise between giving the most number of satellite match ups against proximity to the sampling location. The only exception was for the station at Ulaan Uul, which lies within the Gobi Desert. In this case, the monthly average of the whole scene was used, since the region is only 8.0° × 18.0° wide in the zonal and meridional directions.

Inspection of the time series of the ground based and SCIAMACHY measurements reveals that the in-situ observations are always about 2–4% larger than those observed from space (see Figs. 9 and 10). By only considering the CO₂ anomalies against one another this offset, for the most part, can be effectively removed. Thus, only a comparison between the CO₂ anomalies is feasible.

Of all the sampling sites, the Ulaan Uul anomaly agrees best with the column VMRs measured by SCIAMACHY. The correlation is 0.95 with the phasing and amplitude of the seasonal cycle matching exceptionally well. More importantly the seasonal cycle that SCIAMACHY observes does not simply follow the input a priori column VMRs (as indicated by the green lines in Figs. 9). In addition to Ulaan Uul, there is also excellent agreement at Deuselbach and Schauinsland which have correlation coefficients of 0.90 and 0.83 respectively. At Deuselbach, the agreement between SCIAMACHY and the surface anomalies during March–July is impressive. Furthermore, over both of these sites SCIAMACHY detects a seasonal cycle amplitude which is approximately the same as that at the surface (Table 4). These locations, which are close to one another, both show a small peak in August. Unfortunately, there aren't SCIAMACHY retrievals available for this month, due to instrument decontamination, to corroborate this event. Over Mace Head, Neuglobsow and Plateau Rosa the anomalies agree less well. However, the comparison at both Mace Head and Neuglobsow is hampered as there

[Title Page](#)[Abstract](#)[Introduction](#)[Conclusions](#)[References](#)[Tables](#)[Figures](#)[◀](#)[▶](#)[◀](#)[▶](#)[Back](#)[Close](#)[Full Screen / Esc](#)[Printer-friendly Version](#)[Interactive Discussion](#)

are fewer SCIAMACHY observations (i.e. surrounding grid points) over these station. Mace Head is on the coast, thus a higher number of retrievals are discarded, whereas Neuglobsow sits on the eastern edge of the Western Europe scene. The lack of gridded observations to the east of Neuglobsow clearly affects the agreement between SCIAMACHY and the ground based data. Comprehensive sampling and symmetrical spatial averaging of the SCIAMACHY data around each surface site is therefore necessary to avoid the time series being distorted (or influenced) by for example, pollution events, that occur in only one direction relative to the chosen location. Furthermore, the Plateau Rosa station is also at a very high altitude (>3 km) within the Italian Alps. The effect of the surface topography on the SCIAMACHY retrievals is therefore much greater. Nevertheless, the seasonal amplitude measured at this station is similar to that observed by SCIAMACHY. However, in the spring months there appears to be a noticeable phase shift, with the transition from positive to negative occurring about two and a half months earlier for the observed SCIAMACHY signal.

5.3.2 North America

Further to the study outlined in Sect. 5.3.1, a comparison between two consecutive years (2003–2004) of SCIAMACHY CO₂ measurements to WDCGC surface data over North America was also conducted. Whilst there are numerous operational sampling stations in North America, only four locations (within the USA) were deemed suitable for this assessment. These sites were selected on the basis of having the most number of collocated retrievals to give a more complete time series of SCIAMACHY observations. Owing to the much larger scene observed, as compared to Western Europe, the collocation limits were expanded to $\pm 5.0^\circ$ latitude and $\pm 5.0^\circ$ longitude of each location.

Of the four sites considered, Niwot Ridge, despite its high altitude, yields the best agreement to SCIAMACHY with a correlation coefficient of 0.91 and a similar seasonal cycle amplitude of ~ 9 ppmv (Table 4 and Fig. 12). The phasing between the two observed seasonal cycles is also very similar. However, at this location the a priori closely follows the surface measurements. Similarly, at Wendover the correlation

Title Page

Abstract

Introduction

Conclusions

References

Tables

Figures

◀

▶

◀

▶

Back

Close

Full Screen / Esc

Printer-friendly Version

Interactive Discussion

between SCIAMACHY and the surface observations is high and seasonal amplitudes comparable but again the a priori and surface signals are much alike. At Park Falls and Point Arena the agreement is worse. In spite of this, the observations made at Park Falls are important as they demonstrate that SCIAMACHY detects a seasonal signal that is more similar to the surface observations than the a priori (this is also evident for the Park Falls tower measurements shown in Fig. 13). As the surface albedo tends to be higher at Niwot Ridge and Wendover, than at Park Falls, the signal to noise ratio of the SCIAMACHY measurements is better and the FSI retrievals more accurate at these locations. Thus, it is more likely that observed SCIAMACHY signals at Niwot Ridge and Wendover are realistic and not simply the case that the retrievals are following the a priori. The poor match at Point Arena is most likely to arise from its coastal location and the constraint that only SCIAMACHY observations over land are considered.

To complement these comparisons, tower data taken from the NOAA/ESRL network and the Sylvania tower, in Michigan, was also evaluated against SCIAMACHY CO₂. Each tower measures the CO₂ volume mixing ratio at several different heights with a sampling interval, ranging from minutes to hourly, differing between individual sites (see e.g. Bakwin and Tans, 1995 or Desai et al., 2005). For each tower, CO₂ volume mixing ratio was averaged over all the intake heights and then assembled into a monthly mean time series. The only exception was the Sylvania tower, where the maximum intake height (36 m) was used instead. The resultant time series were then compared to SCIAMACHY observations using the same collocation limits as for the surface measurements. With the exception of Park Falls, where the correlation is 0.92, the agreement between SCIAMACHY and the tower measurements is not noteworthy. This is irrespective of the fact that the magnitude of signal cycle amplitudes are very similar (bar the tower at Argyle where a SCIAMACHY outlier in December distorts the amplitude). At Park Falls however, SCIAMACHY agrees with the tower data much better than with the CO₂ measurements made at the surface. For example, there is especially good agreement in the summer months of 2004 where the changes in the mean CO₂ volume mixing ratios are captured well by SCIAMACHY. The strong corre-

[Title Page](#)[Abstract](#)[Introduction](#)[Conclusions](#)[References](#)[Tables](#)[Figures](#)[I◀](#)[▶I](#)[◀](#)[▶](#)[Back](#)[Close](#)[Full Screen / Esc](#)[Printer-friendly Version](#)[Interactive Discussion](#)

lation is most likely a consequence of the fact that the Park Falls tower measurements can be representative of the entire (well-mixed) PBL (Bakwin and Tans, 1995). At the Sylvania tower, which is quite close to Park Falls, the correlation is not as strong owing to a slight phase difference relative to the time series of SCIAMACHY observations and possibly also because of the low CO₂ intake height. The incomplete tower time series at Argyle coupled with the sites proximity to the eastern coast contribute to the poor correlation with the time series observed by SCIAMACHY.

5.4 Summary

Evaluating the FSI CO₂ retrievals against the ground based observations has demonstrated that SCIAMACHY seems able to detect monthly changes in surface CO₂ concentrations. Out of the seventeen time series comparisons (including those of the aircraft), eleven have correlation coefficients of 0.7 or greater and moreover comparable seasonal cycle amplitudes. At locations where the agreement to SCIAMACHY is poor, mitigating circumstances such as high site altitude or proximity to the coast, or scene edge, are the probable cause. Whilst the simulations in Sect. 5.1 suggest that SCIAMACHY should see a seasonal signal smaller than that at the surface, observations indicate otherwise. It could be possible that SCIAMACHY is simply over estimating the seasonal cycle, owing to some problem with the retrieval itself. Additionally, at Niwot Ridge and Wendover the a priori is similar to the seasonal signal that SCIAMACHY detects, which might indicate that the retrievals are biased from the input data. However, the phasing and changes in the CO₂ anomalies, for example at Deuselbach or the Park Falls tower where smooth seasonal cycles do not occur, match that well that this cannot be the case. Furthermore, it must be remembered that the same a priori CO₂ data has been used in the SCIAMACHY retrievals at all these locations. Thus, the good agreement at Ulln Uul, Deuselbach and Niwot Ridge, which have very different seasonal signals, cannot all be attributed to the a priori. Hence, it is therefore clear that SCIAMACHY is apparently sensitive to the lower troposphere and that surface data can be used as a useful validation proxy for satellite column measurements when considering

Title Page

Abstract

Introduction

Conclusions

References

Tables

Figures

◀

▶

◀

▶

Back

Close

Full Screen / Esc

Printer-friendly Version

Interactive Discussion

only variations in the monthly CO₂ means rather than absolute magnitudes.

6 Case study: North America

6.1 Spatial distributions

The two years of SCIAMACHY data processed by the FSI algorithm over North America allows the inter-annual variability of the retrieved CO₂ spatial distributions to be examined (Figs. 14 and 15). Despite using a different set of a priori data (i.e. 2004 ECMWF and CO₂ data) within the algorithm, there are quite startling coincidences between monthly scenes of each year. This is highly encouraging. For example, in both years during April a thin band of high CO₂ VMRs are witnessed at high latitudes over Ellesmere Island whilst the position of a small localized enhancement over Wyoming (approximately 45° N, 107° E) in 2003, is in the same location as a much more widespread enhancement in 2004. In May, for there are coincidental low CO₂ VMRs over the Appalachian Mountains and southern eastern states which by July develops into significant band of very low CO₂ along the eastern US and also up along the Canadian Shield (though to a lesser extent in 2004). By September, as vegetation photosynthesis is weakening, the CO₂ distributions are much more uniform although there are localized regions of low VMRs e.g. along the Newfoundland Coast or over the Saskatchewan Province in (central) Canada. During October and November, of both years, the retrieved CO₂ fields are again very uniform.

The regional patterns within the 2003-2004 North America CO₂ distributions raises several questions. For instance, are these features real, i.e. do the distributions contain the signature of surface fluxes? Can the CO₂ enhancements and depletions be related to surface processes such as CO₂ emissions or photosynthetic activity, or are they simply a residual surface albedo effect?

There are two arguments for eliminating a possible (seasonal) surface reflectance bias. Firstly, an a priori albedo, determined from the mean radiance of each individual

Title Page

Abstract

Introduction

Conclusions

References

Tables

Figures

◀

▶

◀

▶

Back

Close

Full Screen / Esc

Printer-friendly Version

Interactive Discussion

SCIAMACHY observation, is used within the FSI algorithm to generate each reference spectra. A comparison of the monthly gridded a priori surface albedo (not shown) to the retrieved CO₂ VMRs reveals that whilst the CO₂ distributions evolve considerably with time the a priori albedo shows little variation. Secondly, the comparison between AIRS and SCIAMACHY performed by Barkley et al. (2006b) demonstrated that over North America both instruments essentially observe the same large scale features. With AIRS being a thermal IR instrument, the surface albedo has negligible effect on the data, thus the CO₂ variability arises from changes in its atmospheric concentration. If SCIAMACHY observes the same features, when accounting for surface reflectance within the retrieval, then it too must be observing the same fluctuations in the column integral.

6.2 Correlation with vegetation type

In this section the correlation between the spatial distribution of SCIAMACHY CO₂ and land vegetation cover is explored by comparing SCIAMACHY measurements to five different indicators of vegetation activity at twenty-four different locations in the US (listed in Table 5). The vegetation proxies were taken from the MODerate resolution Imaging Spectroradiometer (MODIS) ASCII subset products³ which are extracted from the global land products for a 7 km×7 km area centred on selected flux towers or field sites located around the world. The MODIS instrument measures light in 36 spectral channels (non-continuously) over a wavelength interval of 0.4–14.4 μm. Two channels are imaged at a nominal ground resolution of 250 m at nadir, five channels at 500 m and the other 29 bands at 1 km. The instrument's mirror has a ±55° scanning pattern which yields a swath of 2330 km (cross track) by 10 km (along track at nadir). Global coverage is achieved every one to two days. The MODIS vegetation data used in this comparison are:

– *Normalized Difference Vegetation Index (NDVI)*

³Downloadable from <http://www.modis.ornl.gov/modis/index.cfm>.

Title Page

Abstract

Introduction

Conclusions

References

Tables

Figures

◀

▶

◀

▶

Back

Close

Full Screen / Esc

Printer-friendly Version

Interactive Discussion

[Title Page](#)
[Abstract](#)[Introduction](#)[Conclusions](#)[References](#)[Tables](#)[Figures](#)[◀](#)[▶](#)[◀](#)[▶](#)[Back](#)[Close](#)[Full Screen / Esc](#)[Printer-friendly Version](#)[Interactive Discussion](#)

EGU

Vegetation is a strong absorber of visible radiation, except for green light ($\lambda=510\text{ nm}$), which is in contrast to NIR radiation which is mostly reflected and scattered by the canopy foliage. The Normalized Difference Vegetation Index (NDVI) is a chlorophyll sensitive index that uses a normalized ratio, between the red and NIR wavelengths, to determine both the presence and condition of vegetation within a satellite footprint:

$$NDVI = \frac{\rho_{NIR} - \rho_{red}}{\rho_{NIR} + \rho_{red}} \quad (4)$$

where ρ_{red} and ρ_{NIR} are the surface bidirectional reflectance factors of the respective MODIS red and NIR bands (Huete et al., 1999). Whilst the NDVI has widely used for operational monitoring (see Huete et al. (2002) and references therein) and provides a long term (20+ year) indicator of vegetation activity it can suffer from atmospheric contamination (e.g. aerosols), saturation over areas of high biomass and is sensitive to variations in the canopy background (Huete et al., 2002). The NDVI product used in this analysis is from the MOD13A2 product which is 16-day composite at 1 km resolution.

– Enhanced Vegetation Index (EVI)

The EVI was developed to counter the problematic effects of the NDVI by normalizing the reflectance in the red band by that in the blue band:

$$EVI = G \times \frac{\rho_{NIR} - \rho_{red}}{\rho_{NIR} + (C_1 \times \rho_{red} - C_2 \times \rho_{blue}) + L} \quad (5)$$

where ρ_{red} , ρ_{NIR} and ρ_{blue} are the atmospherically corrected surface reflectances, L is the canopy background adjustment (to account for radiative transfer through the canopy), G is a gain term (~ 2.5) and C_1 and C_2 are coefficients to correct for the presence of aerosols (Huete et al., 1999).

Title Page

Abstract

Introduction

Conclusions

References

Tables

Figures

◀

▶

◀

▶

Back

Close

Full Screen / Esc

Printer-friendly Version

Interactive Discussion

The advantage of the EVI, compared to the NDVI, is that is more sensitive to the canopy structure rather than chlorophyll content. The EVI is less affected therefore from atmospheric and canopy background contamination and has increased sensitivity (i.e. less saturation) at high biomass levels. The EVI is also taken from the MOD13A product.

– The Fraction of Photosynthetically Absorbed Radiation (FPAR)

FPAR is a measure of the fraction of available radiation, in photosynthetically active wavelengths (400 to 700 nm), that a vegetation canopy absorbs. FPAR is derived (by the MODIS algorithm) from the atmospherically corrected surface reflectance using coupled atmospheric and surface radiative transfer models (Knyazikhin et al., 1999). The FPAR data is taken from the MOD15A2 product which is at 1 km spatial resolution and over an 8-day period.

– Leaf Area Index (LAI)

LAI, also taken from the MOD15A2 product, is a biophysical parameter that describes the structure of the vegetation canopy and is defined as one sided leaf area per unit ground area (Knyazikhin et al., 1999):

$$LAI = \frac{1}{X_s \cdot Y_s} \int_V u_L(r) dr \tag{6}$$

where V is the canopy domain in a given plant is located, X_s and Y_s are the horizontal dimensions of V and $u_L(r)$ is a 3-D leaf area distribution function which describes the heterogeneity of the canopy. The LAI is derived using complex radiative transfer models and is non-linearly related to the FPAR.

– Gross Primary Production (GPP)

The GPP, expressed as the mass of carbon per square metre, can be estimated in very simplistic terms, by multiplying FPAR by the amount of photosynthetically

active radiation (PAR) and then by a conversion efficiency factor ε which represents how much radiation is converted in to plant biomass (Running et al., 1999). The GPP data is taken from the MOD17A2 data and is a composite over an 8-day period.

5 The ground sites were chosen, out of the complete network, to a give widespread geographical coverage and also to incorporate a wide variety of land cover types (see Fig. 16 and Table 5). Each vegetation proxy was smoothed with a 5 point moving average and plotted against the corresponding SCIAMACHY time series, constructed from taking the mean of all monthly gridded CO₂ data lying within $\pm 5.0^\circ$ latitude and $\pm 5.0^\circ$ longitude of each site. Although these collocation limits for SCIAMACHY are much greater than 7 km \times 7 km boundaries for MODIS, it is necessary to ensure a smoother and more complete CO₂ time series. For NDVI, EVI, FPAR and LAI this comparison was performed over a two year time period (2003–2004) whereas for the GPP product only data for 2003 was available.

15 Examinations of the time series plots (e.g. Fig. 17) reveal that there is a strong anti correlation between the retrieved CO₂ VMRs and each of the vegetation proxies. That is, as the terrestrial biosphere becomes more active, as photosynthesis starts to dominate over respiration, the atmospheric CO₂ tend to a minimum whereas the proxies peak (i.e. there is a six month phase difference). Of the vegetation indices, there is slightly better correlation with the EVI than NDVI, with the strongest agreement at BARC (Maryland), Morgan Monroe State Forest, Park Falls and Howland Forest. These sites are covered by deciduous broadleaf or mixed forests and woody savannas, which have a strong seasonal CO₂ signal. The lowest correlations occur at Shy Oaks (closed shrubland), Sevillea BigFoot (grasslands) and Jasper Ridge (woody savannas) where there is a lack of dense vegetation. This draws attention to the fact that where the VI variability is high the retrieved CO₂ variability is also large, for example at Canaan Valley or Bondville (Table 5). If there is a weak CO₂ seasonal cycle then the variability of the VIs is also small. This is evident at Audubon, Maricopa or any of the locations where the correlation was low. Plotting the amplitude of the CO₂ seasonal

**SCIAMACHY
atmospheric CO₂**

Barkley et al.

Title Page

Abstract

Introduction

Conclusions

References

Tables

Figures

◀

▶

◀

▶

Back

Close

Full Screen / Esc

Printer-friendly Version

Interactive Discussion

cycle measured by SCIAMACHY against the respective seasonal amplitudes of the VIs (Fig. 18) illustrates this well as there are not any low VI/high CO₂ or high VI/low CO₂ combinations. The correlation between the SCIAMACHY CO₂ and the NDVI and EVI seasonal amplitudes are significant at 0.56 and 0.68 respectively.

5 Very similar trends are found for the time series of FPAR and LAI (not shown) with the best correlations with SCIAMACHY CO₂ occurring at Canaan Valley, Goodwin Creek, Morgan Monroe State Forest and Park Falls and the worst at Shy Oaks, Sevillea Big-Foot and Jasper Ridge (i.e. in the same locations as the VI correlations). The variability of FPAR and LAI is also closely linked to the CO₂ variability. This is evident at Shy
10 Oaks and Sevillea where there is minimal seasonal variability in CO₂ or either proxy. That aside, the correlation of the FPAR and LAI seasonal amplitudes against the retrieved CO₂ signal is worse than as found for the VIs, being 0.25 and 0.30 respectively (Fig. 18).

The correlation for each between the MODIS GPP and SCIAMACHY CO₂ time series are very similar ~0.3–0.5 and are noticeably lower than as found for NDVI, EVI, FPAR and LAI. For the GPP, the best correlations occur at Niwot Ridge and GLEES, Wyoming, whereas the worst are at Mircopa, Arizona (positive correlation) and Shy
15 Oaks. The correlation between the GPP seasonal amplitude and CO₂ is also significant at 0.59.

20 From this preliminary comparison it can therefore be concluded that SCIAMACHY CO₂ correlates reasonably with the terrestrial biosphere, with low vegetation activity equating to low CO₂ variability. For a more complete analysis, climatological variables such as temperature and precipitation which affect plant growth, also need to be included. However, greater sampling by SCIAMACHY and improvements to FS1
25 retrievals are need to reduce the collocation limits before such a more detailed point analysis can be undertaken. Nevertheless this study is encouraging since it indicates the potential for combining SCIAMACHY atmospheric data and MODIS land products in the future to help investigate the behaviour of the terrestrial biosphere.

[Title Page](#)[Abstract](#)[Introduction](#)[Conclusions](#)[References](#)[Tables](#)[Figures](#)[I◀](#)[▶I](#)[◀](#)[▶](#)[Back](#)[Close](#)[Full Screen / Esc](#)[Printer-friendly Version](#)[Interactive Discussion](#)

7 Conclusions

One of the major issues regarding the retrieval of atmospheric CO₂ from space is the subject of near surface sensitivity. In this paper, SCIAMACHY CO₂ retrieved using the FSI algorithm has been compared to a variety of in situ CO₂ measurements to assess the instruments sensitivity to the lower troposphere and planetary boundary layer. Initial validation, of the daily average CO₂ VMR, against FTS column measurements made at Park Falls, Wisconsin, during 2004 reveal a negative bias of approximately -2% when using SCIAMACHY observations lying within ±1° longitude and latitude of the site. However, this bias becomes smaller if the collocation criteria is relaxed as more SCIAMACHY observations can be used in the calculation of the daily mean. The collocation limits selected also affect the ability of SCIAMACHY to detect day to day variability. As the collocation limits are expanded then the daily variability is captured better, whereas if they are reduced, monthly timescales must be considered instead.

The comparisons to the aircraft measurements over Siberia and to the surface and tower measurements demonstrate that SCIAMACHY is capable of observing the variability of lower tropospheric and surface CO₂. Whilst there is always a negative offset to the absolute magnitudes, the monthly anomalies of SCIAMACHY and the surface stations often agree well and are not believed to be biased by the input a priori CO₂ data. When discrepancies do occur, poor sampling around the site is the most attributable cause.

Additional evidence of the near surface sensitivity of SCIAMACHY is demonstrated by the significant correlations with the MODIS vegetation indices, that are representative of terrestrial vegetation activity over the selected US locations. At many sites, low (or high) vegetation activity is often allied to correspondingly to low (or high) CO₂ variability. As the seasonal variability of vegetation affects the surface reflectance, SCIAMACHY CO₂ retrievals might be biased by vegetation activity. However, the comparison between SCIAMACHY and AIRS CO₂ over North America by [Barkley et al. \(2006b\)](#), indicated that the SCIAMACHY retrievals are not biased by the seasonal vari-

Title Page

Abstract

Introduction

Conclusions

References

Tables

Figures

◀

▶

◀

▶

Back

Close

Full Screen / Esc

Printer-friendly Version

Interactive Discussion

ation in surface albedo. Hence, SCIAMACHY has the potential ability to observe variations in lower tropospheric CO₂ that arise from terrestrial vegetation activity i.e. to detect surface CO₂ fluxes. However, as the validation against the FTS measurements at Park Falls demonstrated, improvements to the FSI retrieval algorithm must be made to remove any negative biases and to improve the precision of the CO₂ observations to more firmly establish the capability of SCIAMACHY for surface flux detection.

Acknowledgements. The authors would like to thank all those involved with the SCIAMACHY instrument especially J. Burrows and the team at IUP/IFE Bremen. We are also grateful to A. Rozanov for supplying the radiative transfer model SCIATRAN. We would like to thank ESA and SRON for supplying the SCIAMACHY data and additionally R. van Hees (of SRON). Thanks also to R. Washenfelder, G. Aleks, G. Toon, and P. Wennberg at Caltech and NASA JPL for the provision of the Park Falls FTS measurements which were obtained with support from NASA. We also are grateful to British Atmospheric Data Centre (BADC) for supplying the ECMWF operational data set. Furthermore, the authors would collectively like to thank all the data providers at each CO₂ sampling station and their respective funding partners and both the NOAA/ESRL and WDCGG networks. The authors finally wish to thank the Natural Environment Research Council (NERC) and CASIX (the Centre for observation of Air-Sea Interactions and fluxes) for supporting M. Barkley through grant ref: NER/S/D/200311751 and NERC and the Data Assimilation Research Council (DARC) for supporting A. Hewitt through grant ref: NER/S/A/2005/13330.

References

- Bakwin, P. S. and Tans, P. P.: Measurements of carbon dioxide on a very tall tower, *Tellus*, 47B, 535–549, 1995. [2484](#), [2493](#), [2494](#)
- Barkley, M. P., Frieß, U., and Monks, P. S.: Measuring atmospheric CO₂ from space using Full Spectral Initiation (FSI) WFM-DOAS, *Atmos. Chem. Phys.*, 6, 3517–3534, 2006a. [2480](#), [2482](#), [2487](#)
- Barkley, M. P., Monks, P. S., and Engelen, R. J.: Comparison of SCIAMACHY and AIRS CO₂ measurements over North America during the summer and autumn of 2003, *Geophys. Res. Lett.*, 33, L20805, doi:10.1029/2006GL026807, 2006b. [2480](#), [2482](#), [2496](#), [2501](#)

Title Page

Abstract

Introduction

Conclusions

References

Tables

Figures

◀

▶

◀

▶

Back

Close

Full Screen / Esc

Printer-friendly Version

Interactive Discussion

**SCIAMACHY
atmospheric CO₂**

Barkley et al.

Title Page

Abstract

Introduction

Conclusions

References

Tables

Figures

◀

▶

◀

▶

Back

Close

Full Screen / Esc

Printer-friendly Version

Interactive Discussion

- Barkley, M. P., Monks, P. S., Frieß, U., Mittermeier, R. L., Fast, H., Körner, S., and Heimann, M.: Comparisons between SCIAMACHY atmospheric CO₂ retrieved using (FSI) WFM-DOAS to ground based FTIR data and the TM3 chemistry transport model, *Atmos. Chem. Phys.*, 6, 4483–4498, 2006c. [2480](#), [2482](#), [2484](#), [2486](#), [2490](#), [2513](#)
- 5 Bösch, H., Toon, G. C., Sen, B., Washenfelder, R., Wennberg, P. O., Buchwitz, M., de Beek, R., Burrows, J. P., Crisp, D., Christi, M., Connor, B. J., Natraj, V., and Yung, Y. L.: Space-based Near-Infrared CO₂ Retrievals: Testing the OCO Retrieval and Validation Concept Using SCIAMACHY Measurements over Park Falls, Wisconsin, *J. Geophys. Res.*, 111, D23302, doi:10.1029/2006JD007080, 2006. [2485](#), [2486](#)
- 10 Bovensmann, H., Burrows, J. P., Buchwitz, M., Frerick, J., Noël, S., Rozanov, V. V., Chance, K. V., and Goede, A.: SCIAMACHY – mission objectives and measurement modes, *J. Atmos. Sci.*, 56, 127–150, 1999. [2481](#)
- Buchwitz, M., Rozanov, V. V., and Burrows, J. P.: A near infrared optimized DOAS method for the fast global retrieval of atmospheric CH₄, CO, CO₂, H₂O, and N₂O total column amounts from SCIAMACHY/ENVISAT-1 nadir radiances, *J. Geophys. Res.*, 105, 15 231–15 246, 2000. [2482](#)
- 15 Buchwitz, M., de Beek, R., Burrows, J. P., Bovensmann, H., Warneke, T., Notholt, J., Meirink, J. F., Goede, A. P. H., Bergamaschi, P., Körner, S., Heimann, M., and Schulz, A.: Atmospheric methane and carbon dioxide from SCIAMACHY satellite data: initial comparison with chemistry and transport models, *Atmos. Chem. Phys.*, 5, 941–962, 2005a. [2480](#)
- Buchwitz, M., de Beek, R., Noël, S., Burrows, J. P., Bovensmann, H., Bremer, H., Bergamaschi, P., Körner, S., and Heimann, M.: Carbon monoxide, methane and carbon dioxide columns retrieved from SCIAMACHY by WFM-DOAS: year 2003 initial data set, *Atmos. Chem. Phys.*, 5, 3313–3329, 2005b. [2480](#), [2483](#)
- 20 Buchwitz, M., de Beek, R., Noël, S., Burrows, J. P., Bovensmann, H., Schneising, O., Khlystova, I., Bruns, M., Bremer, H., Bergamaschi, P., Körner, S., and Heimann, M.: Atmospheric carbon gases retrieved from SCIAMACHY by WFM-DOAS: version 0.5 CO and CH₄ and impact of calibration improvements on CO₂ retrieval, *Atmos. Chem. Phys.*, 6, 2727–2751, 2006, <http://www.atmos-chem-phys.net/6/2727/2006/>. [2480](#), [2483](#)
- 25 Desai, A. R., Bolstad, P., Cook, B. D., Davis, K. J., and Carey, E. V.: Comparing net ecosystem exchange of carbon dioxide between an old-growth and mature forest in the upper MidWest, USA, *Agric. Forest Meteorol.*, 128, 33–35, 2005. [2493](#)
- 30 Dils, B., De Mazière, M., Müller, J. F., Blumenstock, T., Buchwitz, M., de Beek, R., De-

**SCIAMACHY
atmospheric CO₂**

Barkley et al.

Title Page

Abstract

Introduction

Conclusions

References

Tables

Figures

◀

▶

◀

▶

Back

Close

Full Screen / Esc

Printer-friendly Version

Interactive Discussion

moulin, P., Duchatelet, P., Fast, H., Frankenberg, C., Gloude-mans, A., Griffith, D., Jones, N., Kerzenmacher, T., Kramer, I., Mahieu, E., Mellqvist, J., Mittermeier, R. L., Notholt, J., Rinsland, C. P., Schrijver, H., Smale, D., Strandberg, A., Straume, A. G., Stremme, W., Strong, K., Sussmann, R., Taylor, J., van den Broek, M., Velazco, V., Wagner, T., Warneke, T., Wiacek, A., and Wood, S.: Comparisons between SCIAMACHY and ground-based FTIR data for total columns of CO, CH₄, CO₂ and N₂O, Atmos. Chem. Phys., 6, 1953–1976, 2006, <http://www.atmos-chem-phys.net/6/1953/2006/>. 2484

Engelen, R. J. and McNally, A. P.: Estimating atmospheric CO₂ from advanced infrared satellite radiances within an operational four-dimensional variational (4D-Var) data assimilation system: Results and validation, J. Geophys. Res., 110, D18305, doi:10.1029/2005JD005982, 2005. 2480

Gloude-mans, A. M. S., Schrijver, H., Kleipool, Q., van den Broek, M. M. P., Straume, A. G., Lichtenberg, G., van Hees, R., Aben, I., and Meirink, J. F.: The impact of SCIAMACHY near-infrared instrument calibration on CH₄ and CO total columns, Atmos. Chem. Phys., 5, 2369–2383, 2005, <http://www.atmos-chem-phys.net/5/2369/2005/>. 2484

Gottwald, M., Bovensmann, H., Lichtenberg, G., Noël, S., von Bergen, A., Slijkhuis, S., PETERS, A., Hoogeveen, R., von Savigny, C., Buchwitz, M., Kokhanovsky, A., Richter, A., Rozanov, A., Holzer-Popp, T., Bramstedt, K., Lambert, J.-C., Skupin, J., Wittrock, F., Schrijver, and Burrows, J. P.: SCIAMACHY Monitoring the Earth's Changing Atmosphere, DLR, Insitut für Methodik der Fernerkundung (IMF), Germany, 2006. 2481

Gurney, K. R., Law, R. M., Denning, A. S., Rayner, P. J., Baker, D., Bousquet, P., Bruhwilerk, L., Chen, Y.-H., Ciais, P., Fan, S., Fung, I. Y., Gloor, M., Heimann, M., Higuchi, K., John, J., Maki, T., Maksyutov, S., Masariek, K., Peylin, P., Pratherkk, M., Pakkk, B. C., Randerson, J., Sarmiento, J., Taguchi, S., Takahashi, T., and Yuen, C.-W.: Towards robust regional estimates of sources and sinks using atmospheric transport models, Nature, 415, 626–630, 2002. 2479

Houweling, S., Brëon, F.-M., Aben, I., Rödenbeck, C., Gloor, M., Heimann, M., and Ciais, P.: Inverse modeling of CO₂ sources and sinks using satellite data: a synthetic inter-comparison of measurement techniques and their performance as a function of space and time, Atmos. Chem. Phys., 4, 523–538, 2004, <http://www.atmos-chem-phys.net/4/523/2004/>. 2479

Houweling, S., Hartmann, W., Aben, I., Schrijver, H., Skidmore, J., Roelofs, G.-J., and Brëon, F.-M.: Evidence of systematic errors in SCIAMACHY-observed CO₂ due to aerosols, Atmos. Chem. Phys., 5, 3003–3013, 2005, <http://www.atmos-chem-phys.net/5/3003/2005/>. 2480

- Huete, A., Justice, C., and van Leeuwen, W.: MODIS Vegetation Index (MOD 13) Algorithm Theoretical Basis Document, 1999. [2497](#)
- Huete, A., Didan, K., Miura, T., Rodriguez, E. P., Gao, X., and Ferreira, L. G.: Overview of the radiometric and biophysical performance of the MODIS vegetation indices, *Remote Sens. Environ.*, 83, 195–213, 2002. [2497](#)
- Kiehl, J. T. and Trenberth, K. E.: Earth's Annual Global Mean Energy Budget, *Bulletin of the American Meteorological Society*, 78, 197–208, 1997. [2479](#)
- Kleipool, Q.: Algorithm Specification for Dark Signal Determination, Tech. rep., SRON-SCIA-30 PhE-RP-009, SRON, 2003a. [2484](#)
- Kleipool, Q.: Recalculation of OPTEC5 Non-Linearity, Report containing the NL correction to be implemented in the data processor, Tech. rep. SRON-SCIA-PhE-RP-013, SRON, 2003b. [2484](#)
- Kneizys, F. X., Abreu, L. W., Anderson, G. P., Shettle, E. P., Chetwynd, J. H., Shettle, E. P., Berk, A., Bernstein, L., Robertson, D., Acharya, P., Rothman, L., Selby, J. E. A., Allery, W. O., and Clough, S. A.: The MODTRAN 2/3 report and LOWTRAN 7 model, Tech. rep., Philips Laboratory, Hanscom AFB, 1996. [2483](#)
- Knyazikhin, Y., Glassy, J., Privette, J. L., Tian, Y., Lotsch, A., Zhang, Y., Wang, Y., Morisette, J. T., Votava, P., Myneni, R. B., and Nemani, S. W. R.: MODIS Leaf Area Index (LAI) And Fraction Of Photosynthetically Active Radiation Absorbed By Vegetation (FPAR) Product (MOD15) Algorithm Theoretical Basis Document Version 4.0, 1999. [2498](#)
- Krijger, J. M., Aben, I., and Schrijver, H.: Distinction between clouds and ice/snow covered surfaces in the identification of cloud-free observations using SCIAMACHY PMDs, *Atmos. Chem. Phys.*, 5, 2279–2738, 2005, <http://www.atmos-chem-phys.net/5/2279/2005/>. [2484](#)
- Machida, T., Nakazawa, T., Muksyutov, S., Tohjima, Y., Takahashi, Y., Watai, T., Vinnichenko, N., Panchenko, M., Arshinov, M., Fedoseev, N., and Inoue, G.: Temporal and spatial variations of atmospheric CO₂ mixing ratio over Siberia, *Proceedings of The Sixth International CO₂ Conference, Sendai, Japan, 2001*. [2488](#)
- O'Brien, D. M. and Rayner, P. J.: Global observations of the carbon budget, 2. CO₂ column from differential absorption of reflected sunlight in the 1.61 μm band of CO₂, *J. Geophys. Res.*, 107, D14354, doi:10.1029/2001JD000617, 2002. [2479](#)
- Patra, P. K., Gurney, K. R., Denning, A. S., Maksyutov, S., Nakazawa, T., Baker, D., Bousquet, P., Bruhwiler, L., Chen, Y.-H., Ciais, P., Fan, S., Fung, I., Gloor, M., Heimann, M., Higuchi, K., John, J., Law, R. M., Maki, T., Pak, B. C., Peylin, P., Prather, M., Rayner, P. J., Sarmiento,

Title Page

Abstract

Introduction

Conclusions

References

Tables

Figures

◀

▶

◀

▶

Back

Close

Full Screen / Esc

Printer-friendly Version

Interactive Discussion

[Title Page](#)[Abstract](#)[Introduction](#)[Conclusions](#)[References](#)[Tables](#)[Figures](#)[◀](#)[▶](#)[◀](#)[▶](#)[Back](#)[Close](#)[Full Screen / Esc](#)[Printer-friendly Version](#)[Interactive Discussion](#)

J., Taguchi, S., Takahashi, T., and Yuen, C.-W.: Sensitivity of inverse estimation of annual mean CO₂ sources and sinks to ocean-only sites versus all-sites observational networks, *Geophys. Res. Lett.*, 33, L05814, doi:10.1029/2005GL025403, 2006. [2479](#)

Remedios, J. J., Parker, R. J., Panchal, M., Leigh, R. J., and Corlett, G.: Signatures of atmospheric and surface climate variables through analyses of infrared spectra (SATSCAN-IR), Proceedings of the first EPS/METOP RAO Workshop, ESRIN, 2006. [2483](#), [2487](#), [2508](#)

Rödenbeck, C., Houweling, S., Gloor, M., and Heimann, M.: CO₂ flux history 1982–2001 inferred from atmospheric data using a global inversion of atmospheric transport, *Atmos. Chem. Phys.*, 3, 1919–1964, 2003, <http://www.atmos-chem-phys.net/3/1919/2003/>. [2479](#)

Rothman, L., Jacquemart, D., Barbe, A., Benner, C. D., Birk, M., Brown, L. R., Carleer, M. R., Chackerian Jr., C., Chance, K., Coudert, L. H., Dana, V., Devi, V. M., Flaud, J.-M., Gamache, R. R., Goldman, A., Hartmann, J.-M., Jucks, J. W., Maki, A. G., Mandin, J.-Y., Massie, S. T., Orphal, J., Perrin, A., Rinsland, C. P., Smith, M., Tennyson, J., Tolchenov, R. N., Toth, R. A., Vander Auwera, J., Varanasi, P., and Wagner, G.: The *HITRAN* 2004 molecular spectroscopic database, *J. Quant. Spectrosc. Radiat. Transfer*, 96, 193–204, 2005. [2483](#)

Ročanov, V. V., Buchwitz, M., Eichmann, K. U., de Beek, R., and Burrows, J. P.: SCIAMACHY – a new radiative transfer model for geophysical applications in the 240–2400 nm spectral region: The pseudo-spherical version, presented at COSPAR 2000, *Adv. Space Res.*, 29(11), 1831–1835, 2002. [2483](#)

Running, S. W., Nemani, R., Glassy, J. M., and Thornton, P. E.: MODIS Daily Photosynthesis (PSN) and annual Net Primary Production (NPP)(MOD17) Algorithm Theoretical Basis Document, 1999. [2499](#)

Siegenthaler, U., Stocker, T. F., Monnin, E., Lüthi, D., Schwander, J., Stauffer, B., Raynaud, D., Barnola, J.-M., Fischer, H., and Valérie Masson-Delmotte, J. J.: Stable Carbon Cycle/Climate Relationship During the Late Pleistocene, *Science*, 310, 1313–1317, 2005. [2479](#)

Tiwari, Y. K., Gloor, M., Engelen, R. J., Chevallier, F., Rödenbeck, C., Körner, S., Peylin, P., Braswell, B. H., and Heimann, M.: Comparing CO₂ retrieved from AIRS with model predictions: implications for constraining surface fluxes and lower-to-upper troposphere transport, *J. Geophys. Res.*, 111, D17106, doi:10.1029/2005JD006681., 2006. [2480](#)

Washenfelder, R. A., Toon, G. C., Yang, Z., Allen, N. T., Wennberg, P. O., Vay, S. A., Matross, D. M., and Daube, B. C.: Carbon dioxide column abundances at the Wisconsin Tall Tower site, *J. Geophys. Res.*, 111, D22305, doi:10.1029/2006JD007154, 2006. [2485](#)

**SCIAMACHY
atmospheric CO₂**

Barkley et al.

Table 1. Summary of the FTS and SCIAMACHY comparison, showing the collocation limits, the number of daily match ups N_C , the mean bias B and its 1σ error, the mean column VMRs, M_{FTS} and M_{SCIA} for the FTS and SCIAMACHY measurements respectively and their corresponding 1σ standard deviations σ_{FTS} and σ_{SCIA} , and finally N_{FSI} which is the number of SCIAMACHY observations used in the calculation of SCIA_M .

Collocation Limits (lon × lat)	N_C [–]	B [%]	σ_B [%]	M_{FTS} [ppmv]	σ_{FTS} [ppmv]	M_{SCIA} [ppmv]	σ_{SCIA} [ppmv]	N_{FSI} [–]	r [–]
0.5° × 0.5°	13	–3.1	2.6	374.4	2.4	362.8	10.8	4	0.54
1.0° × 1.0°	20	–2.1	2.3	374.5	2.1	366.7	9.3	10	0.36
2.0° × 2.0°	26	–1.6	1.8	374.3	2.7	368.2	7.7	24	0.49
3.0° × 3.0°	29	–1.5	1.6	374.5	2.7	369.1	7.8	40	0.73
4.0° × 4.0°	30	–1.3	1.6	374.4	2.7	369.5	7.5	55	0.71
5.0° × 5.0°	34	–1.1	1.4	374.4	2.6	370.2	6.8	69	0.71
10.0° × 10.0°	40	–0.9	1.3	374.4	2.8	371.0	6.2	208	0.68

Title Page

Abstract

Introduction

Conclusions

References

Tables

Figures

◀

▶

◀

▶

Back

Close

Full Screen / Esc

Printer-friendly Version

Interactive Discussion

Table 2. Summary of the simulated seasonal cycle amplitudes for the retrieved and true column VMRs, \hat{V}_{CO_2} and $V_{\text{CO}_2}^t$ respectively, in comparison to the seasonal cycles at the surface and for different altitudes within the lower troposphere when using the CO₂ climatology (Remedios et al., 2006).

Latitude	$V_{\text{CO}_2}^t$	\hat{V}_{CO_2}	Seasonal Cycle Amplitude [ppmv]						
			0 km	1 km	2 km	3 km	4 km	5 km	0–5 km
60–90° N	9.0	11.3	14.7	15.1	14.7	13.3	11.8	11.1	13.4
30–60° N	4.6	5.9	10.5	9.3	8.6	7.0	5.8	5.3	7.4
0–30° N	3.5	4.0	4.3	4.6	5.1	5.3	4.6	3.7	4.7
0–30° S	1.4	1.5	1.7	1.7	1.7	1.6	1.5	1.5	1.6
30–60° S	1.9	1.9	1.9	1.9	1.8	1.9	2.0	2.1	1.9
60–90° S	1.9	2.0	2.2	2.1	2.1	2.1	2.1	2.1	2.1

Title Page

Abstract

Introduction

Conclusions

References

Tables

Figures

◀

▶

◀

▶

Back

Close

Full Screen / Esc

Printer-friendly Version

Interactive Discussion

**SCIAMACHY
atmospheric CO₂**

Barkley et al.

Table 3. Summary of aircraft and SCIAMACHY comparison over Siberia. All values within the table are computed using only coincidental aircraft and SCIAMACHY observations (i.e. when both measurements occur on the same day). The amplitude of the seasonal cycles (SCA) are shown for SCIAMACHY (denoted SCIA) and for the aircraft over its complete sampling altitude range. The correlation between the aircraft and SCIAMACHY CO₂ is also shown in the last column.

Location	Vegetation Type	Number of flights	Altitude Range [km]	SCA [ppmv]		Correlation [-]
				Aircraft	SCIA	
Novosibirsk	Forest	12	0.0–7.0	23.5	21.0	0.79
Surgut	Wetland	12	0.0–7.0	11.0	26.0	0.90
Yakutsk	Forest	20	0.0–3.0	25.0	17.5	0.72

Title Page

Abstract

Introduction

Conclusions

References

Tables

Figures

◀

▶

◀

▶

Back

Close

Full Screen / Esc

Printer-friendly Version

Interactive Discussion

Table 4. Summary of the in-situ ground based comparison over western Europe, Mongolia and the US. The seasonal cycle amplitudes (SCA) are given both the ground based (g-b) and SCIAMACHY (SCIA) observations. The correlation between the time series is also given. Summary of the ground based tower comparison over the USA. The average correlation using all locations is 0.7.

Location	SCA [ppmv]		Correlation [-]
	g-b	SCIA	
Surface:			
Deuselbach, Germany	15.9	17.7	0.90
Mace Head, Eire	11.1	15.3	0.72
Neuglobsow, Germany	17.6	22.7	0.62
Plateau Rosa, Italy	8.6	10.1	0.56
Schauinsland, Germany	13.4	13.7	0.83
Ulaan Uul, Mongolia	11.5	10.6	0.95
Tower:			
Park Falls, Wisconsin, USA	23.1	17.4	0.72
Niwot Ridge, Colorado, USA	9.6	9.4	0.91
Point Arena, California, USA	13.3	8.3	0.39
Wendover, Utah, USA	9.9	11.7	0.85
Argyle, Maine, USA	7.7	30.1	0.19
Park Falls, Wisconsin, USA	18.0	17.4	0.93
Moody, Texas, USA	10.2	9.0	0.50
Sylvania Tower, Michigan, USA	15.9	18.4	0.76

Title Page

Abstract Introduction

Conclusions References

Tables Figures

◀ ▶

◀ ▶

Back Close

Full Screen / Esc

Printer-friendly Version

Interactive Discussion

Table 5. Summary of the comparison between SCIAMACHY and MODIS vegetation indices data. The correlations are between the SCIAMACHY CO₂ monthly averages and the (time interpolated) MODIS index. The vegetation type is taken from the MODIS MOD12Q1 Land Cover product.

Site Index/Name	Vegetation Type	Correlation				
		EVI	NDVI	FPAR	LAI	GPP
1. Audubon Research Ranch, Arizona, USA	Desert/grassland	-0.75	-0.69	-0.72	-0.72	-0.53
2. Beltsville Agricultural Research Center, Maryland	Deciduous broadleaf	-0.92	-0.84	-0.77	-0.91	-0.51
3. Blodgett Forest, California	Evergreen needleleaf forest	-0.26	-0.54	-0.39	-0.36	-0.31
4. Bondville, Illinois	Croplands	-0.85	-0.81	-0.77	-0.74	-0.48
5. Canaan Valley, West Virginia	Cropland/natural mosaic	-0.90	-0.82	-0.84	-0.93	-0.53
6. Chestnut Ridge, Oak Ridge, Tennessee	Deciduous broadleaf	-0.78	-0.76	-0.76	-0.87	-0.50
7. Cub Hill (Baltimore), Maryland	Urban	-0.90	-0.82	-0.75	-0.86	-0.52
8. Duke Forest - loblolly pine, North Carolina	Mixed forests	-0.88	-0.85	-0.68	-0.89	-0.37
9. Florida-Kennedy Space Center (scrub oak)	Evergreen needleleaf forest	-0.86	-0.14	-0.20	-0.80	-0.36
10. Fort Peck, Montana	Grasslands	-0.83	-0.83	-0.36	-0.07	-0.57
11. GLEES, Wyoming	Woody savannas	-0.80	-0.83	-0.79	-0.78	-0.65
12. Goodwin Creek, Mississippi	Cropland/natural mosaic	-0.78	-0.76	-0.85	-0.87	-0.58
13. Harvard Forest EMS Tower, Massachusetts (HFR1)	Mixed forests	-0.88	-0.75	-0.75	-0.83	-0.52
14. Howland Forest (west tower), Maine	Mixed forests	-0.91	-0.78	-0.80	-0.92	-0.51
15. Jasper Ridge, California	Woody savannas	0.36	0.62	0.11	0.32	-0.33
16. Lake Tahoe, Nevada	Woody savannas	-0.80	-0.70	-0.77	-0.79	-0.54
17. Maricopa Agricultural Center, Arizona	Grasslands	-0.78	-0.71	-0.25	-0.43	0.10
18. Metolius-intermediate aged ponderosa pine, Oregon	Evergreen needle leaf forests	-0.01	-0.28	-0.25	-0.27	-0.29
19. Morgan Monroe State Forest, Indiana	Deciduous broadleaf	-0.91	-0.90	-0.81	-0.88	-0.52
20. Niwot Ridge Forest, Colorado (LTER NWT1)	Evergreen needleleaf forests	-0.67	-0.74	-0.71	-0.72	-0.65
21. Park Falls/WLEF, Wisconsin	Woody savannas	-0.92	-0.86	-0.81	-0.92	-0.58
22. Rannells Ranch (ungrazed), Kansas	Grasslands	-0.64	-0.67	-0.63	-0.54	-0.51
23. Sevilleta BigFoot, New Mexico	Grasslands	-0.28	-0.31	-0.45	-0.48	-0.56
24. Sky Oaks, Young Stand, California	Closed shrubland	-0.18	-0.09	-0.35	-0.34	-0.23

SCIAMACHY atmospheric CO₂

Barkley et al.

Title Page

Abstract

Introduction

Conclusions

References

Tables

Figures

◀

▶

◀

▶

Back

Close

Full Screen / Esc

Printer-friendly Version

Interactive Discussion

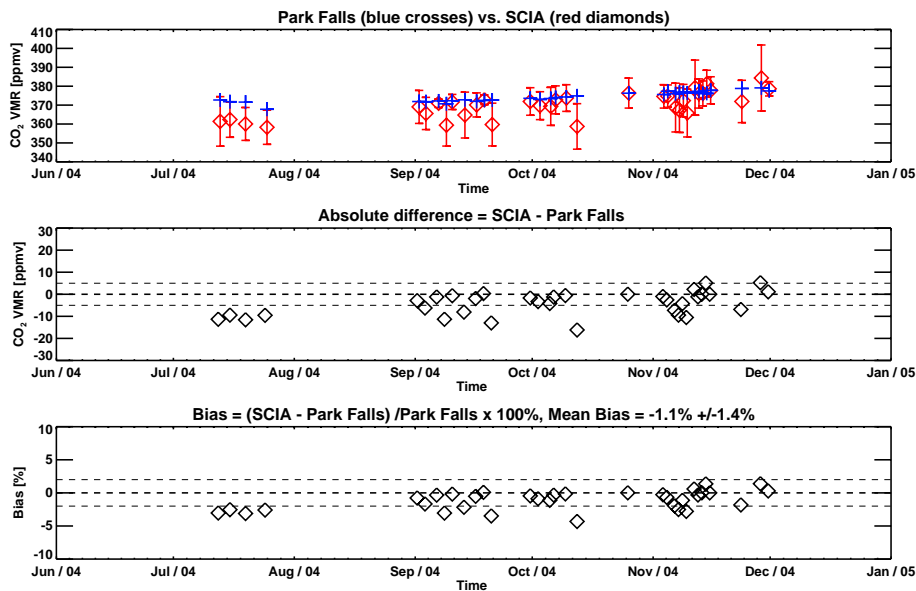


Fig. 1. Top Panel: The daily mean FTS CO₂ column measurements (blue crosses) with the corresponding daily average of all SCIAMACHY measurements (red diamonds) occurring within 5.0°×5.0° of the Park Falls site together with its 1 σ error. Middle Panel: The absolute difference (SCIAMACHY minus FTS) between the satellite and ground based observations. The grey dashed lines indicate the ± 5 ppmv differences. Bottom Panel: The percentage bias of each SCIAMACHY observation with respect to the FTS measurements. The grey dashed lines indicate the $\pm 2\%$ bias threshold.

[Title Page](#)[Abstract](#)[Introduction](#)[Conclusions](#)[References](#)[Tables](#)[Figures](#)[I◀](#)[▶I](#)[◀](#)[▶](#)[Back](#)[Close](#)[Full Screen / Esc](#)[Printer-friendly Version](#)[Interactive Discussion](#)

EGU

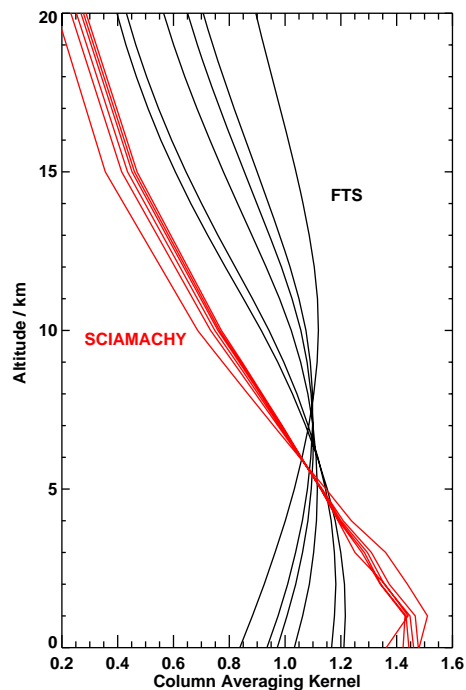


Fig. 2. Example averaging kernels, for various solar zenith angles (i.e. air masses), for SCIAMACHY (red line) and the FTS (black line) highlighting the different sensitivity of each instrument to the lower troposphere. The SCIAMACHY averaging kernels are calculated numerically (see, e.g. [Barkley et al., 2006c](#)).

[Title Page](#)[Abstract](#)[Introduction](#)[Conclusions](#)[References](#)[Tables](#)[Figures](#)[◀](#)[▶](#)[◀](#)[▶](#)[Back](#)[Close](#)[Full Screen / Esc](#)[Printer-friendly Version](#)[Interactive Discussion](#)

EGU

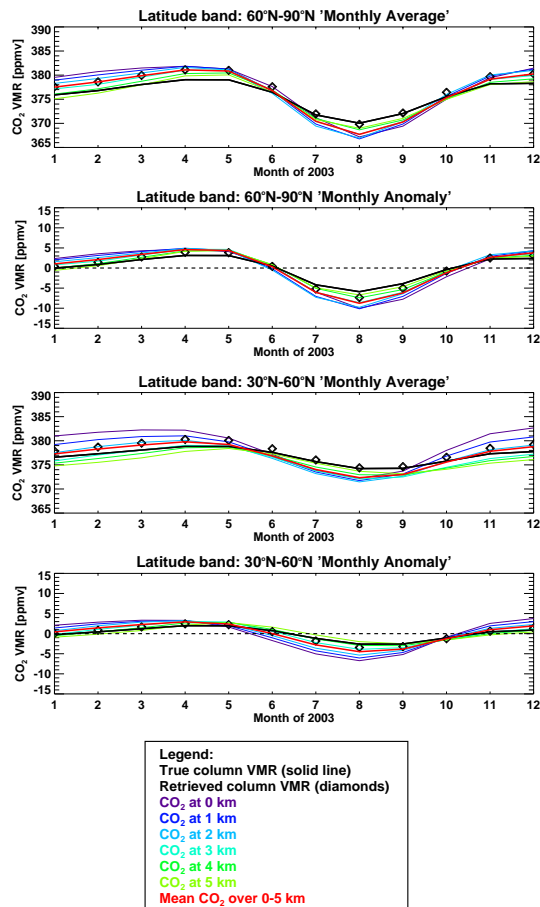


Fig. 3. Assessment of the near surface sensitivity of SCIAMACHY, for different latitude regions, using the 2003 CO₂ climatology. The plots show the the retrieved and true column VMRs against CO₂ mixing ratios within the lower troposphere both in terms of absolute magnitudes and also the anomalies.

[Title Page](#)
[Abstract](#)
[Introduction](#)
[Conclusions](#)
[References](#)
[Tables](#)
[Figures](#)
[◀](#)
[▶](#)
[◀](#)
[▶](#)
[Back](#)
[Close](#)
[Full Screen / Esc](#)
[Printer-friendly Version](#)
[Interactive Discussion](#)

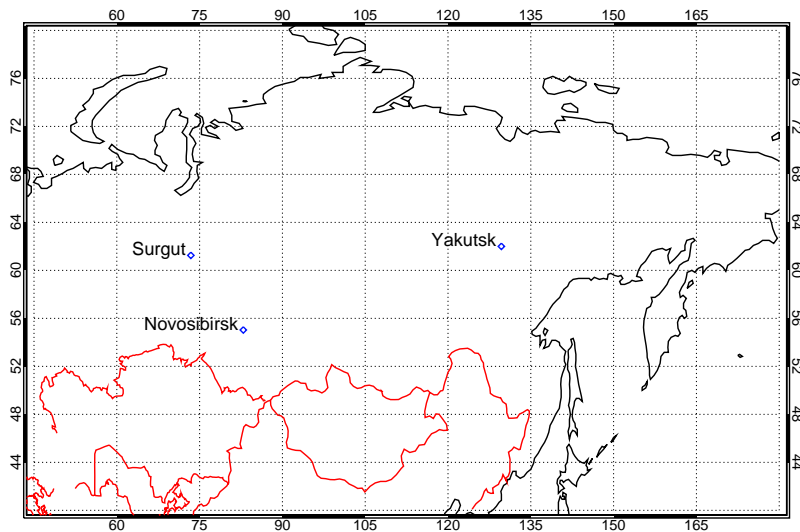


Fig. 4. The locations of the aircraft flights over Siberia during 2003: Novosibirsk (55.03° N, 82.19° E), Surgut (61.25° N, 73.41° E) and Yakutsk (62.00° N, 129.66° E).

[Title Page](#)[Abstract](#)[Introduction](#)[Conclusions](#)[References](#)[Tables](#)[Figures](#)[◀](#)[▶](#)[◀](#)[▶](#)[Back](#)[Close](#)[Full Screen / Esc](#)[Printer-friendly Version](#)[Interactive Discussion](#)

EGU

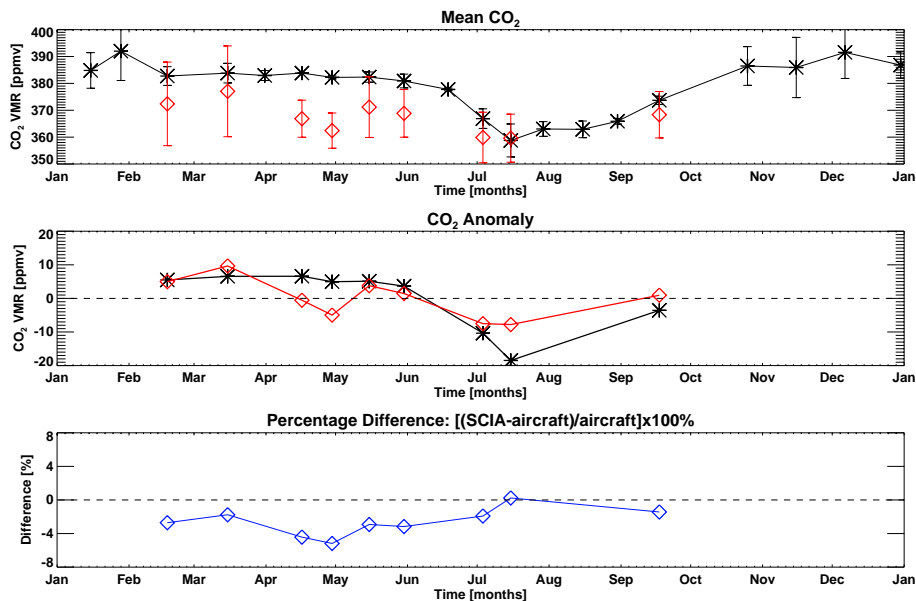


Fig. 5. The CO₂ time series over Yakutsk for SCIAMACHY (red) and aircraft (black). Top panel: The mean aircraft CO₂ mixing ratio (over all altitudes) and the SCIAMACHY VMRs. The error bars represent the 1σ uncertainty. Second panel: The CO₂ anomaly (using only coincidental observations). Third panel: The percentage difference between SCIAMACHY and the mean aircraft CO₂ mixing ratio (over all altitudes).

[Title Page](#)[Abstract](#)[Introduction](#)[Conclusions](#)[References](#)[Tables](#)[Figures](#)[◀](#)[▶](#)[◀](#)[▶](#)[Back](#)[Close](#)[Full Screen / Esc](#)[Printer-friendly Version](#)[Interactive Discussion](#)

EGU

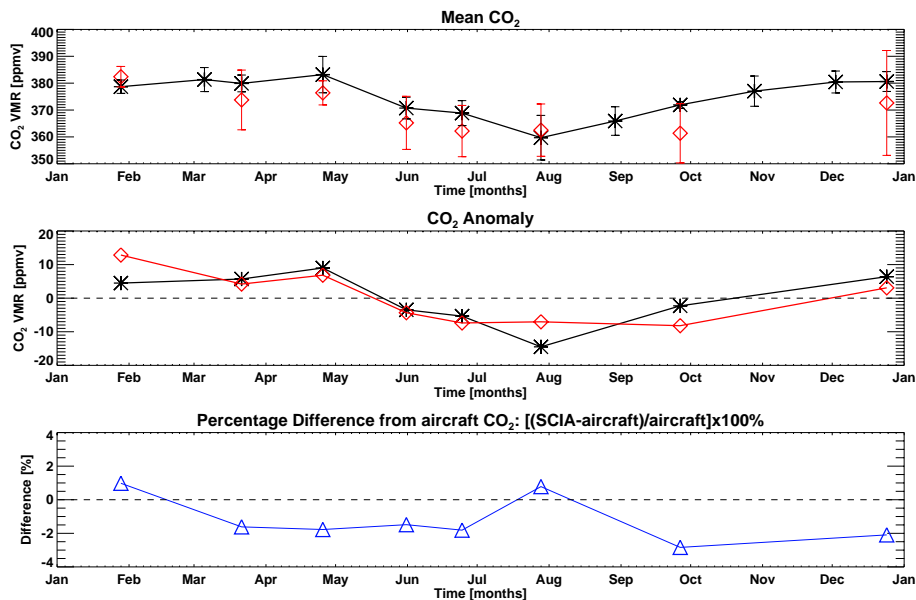


Fig. 6. As Fig. 5 but for the CO₂ time series over Novosibirsk.

[Title Page](#)[Abstract](#)[Introduction](#)[Conclusions](#)[References](#)[Tables](#)[Figures](#)[◀](#)[▶](#)[◀](#)[▶](#)[Back](#)[Close](#)[Full Screen / Esc](#)[Printer-friendly Version](#)[Interactive Discussion](#)

EGU

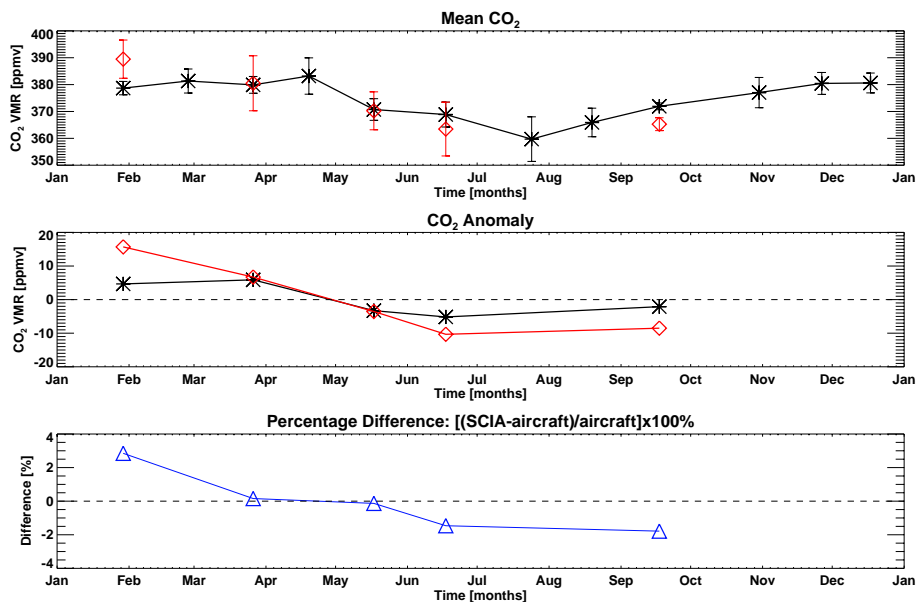


Fig. 7. As Fig. 5 but for the CO₂ time series over Surgut.

[Title Page](#)[Abstract](#)[Introduction](#)[Conclusions](#)[References](#)[Tables](#)[Figures](#)[◀](#)[▶](#)[◀](#)[▶](#)[Back](#)[Close](#)[Full Screen / Esc](#)[Printer-friendly Version](#)[Interactive Discussion](#)

EGU

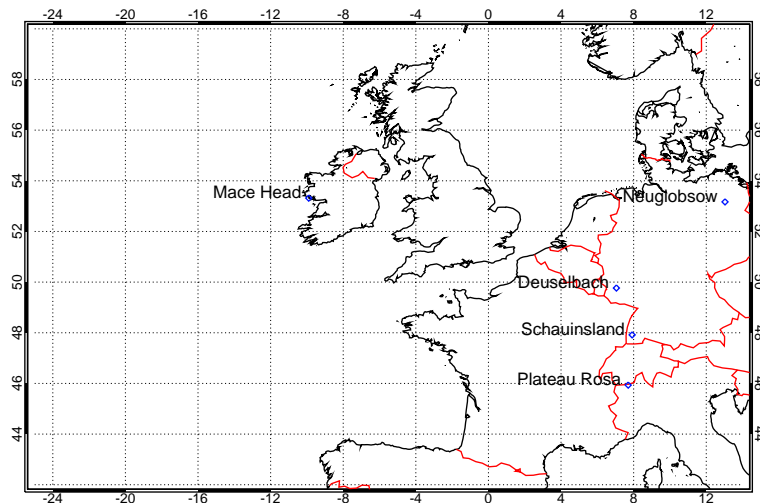


Fig. 8. The surface stations located within the European scene processed by the FSI retrieval algorithm.

[Title Page](#)[Abstract](#)[Introduction](#)[Conclusions](#)[References](#)[Tables](#)[Figures](#)[◀](#)[▶](#)[◀](#)[▶](#)[Back](#)[Close](#)[Full Screen / Esc](#)[Printer-friendly Version](#)[Interactive Discussion](#)

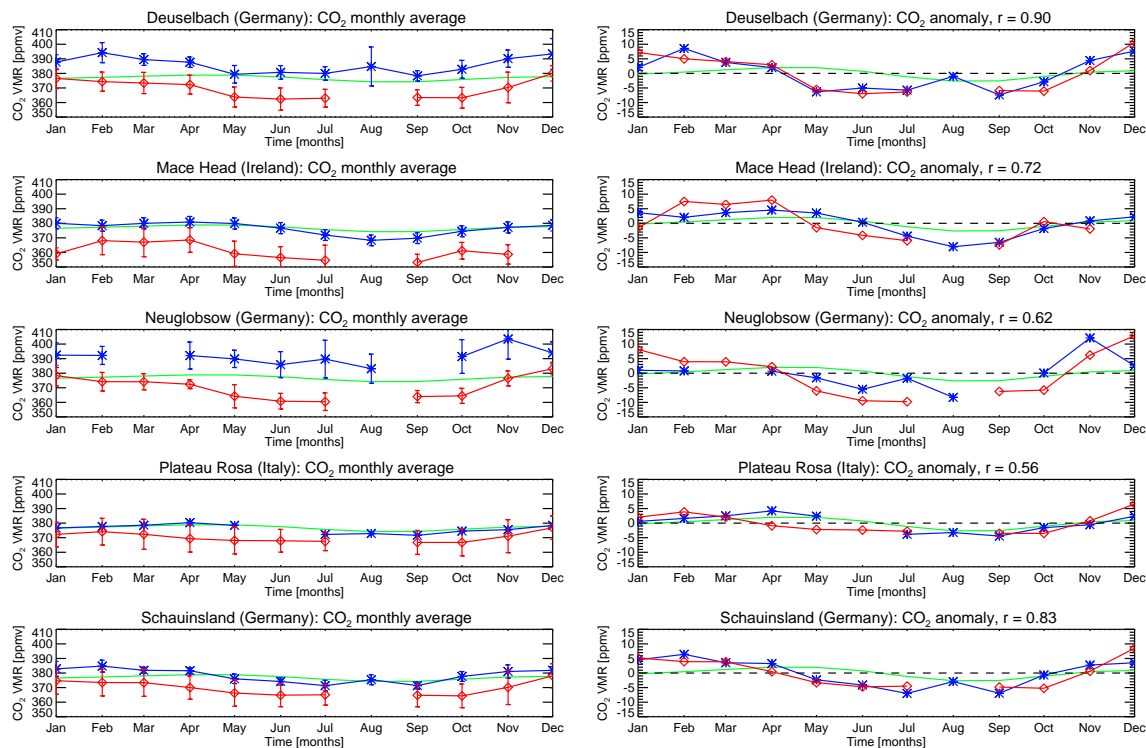


Fig. 9. Time series of ground based European in situ observations (blue) versus SCIAMACHY CO₂ (red). The 1σ error bars are shown on the monthly averages. The a priori CO₂ column VMR is shown in green.

[Title Page](#)
[Abstract](#)
[Introduction](#)
[Conclusions](#)
[References](#)
[Tables](#)
[Figures](#)
[◀](#)
[▶](#)
[◀](#)
[▶](#)
[Back](#)
[Close](#)
[Full Screen / Esc](#)
[Printer-friendly Version](#)
[Interactive Discussion](#)

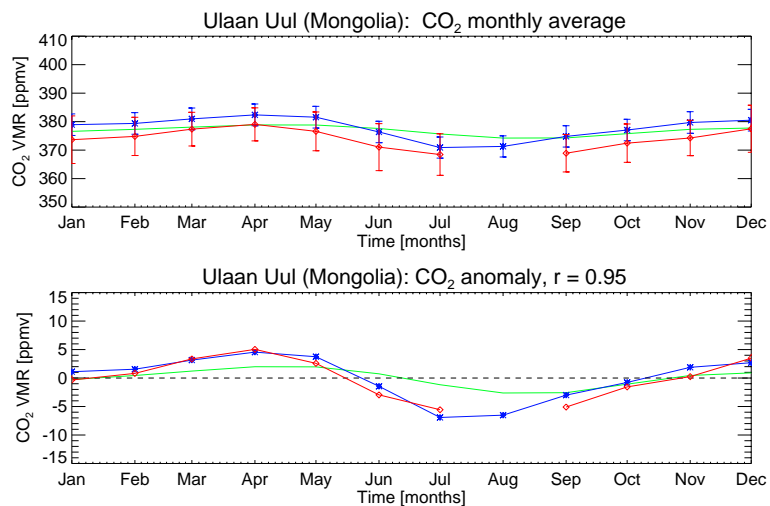


Fig. 10. As Fig. 9 but for Ulaan Uul, Mongolia.

[Title Page](#)[Abstract](#)[Introduction](#)[Conclusions](#)[References](#)[Tables](#)[Figures](#)[◀](#)[▶](#)[◀](#)[▶](#)[Back](#)[Close](#)[Full Screen / Esc](#)[Printer-friendly Version](#)[Interactive Discussion](#)

EGU

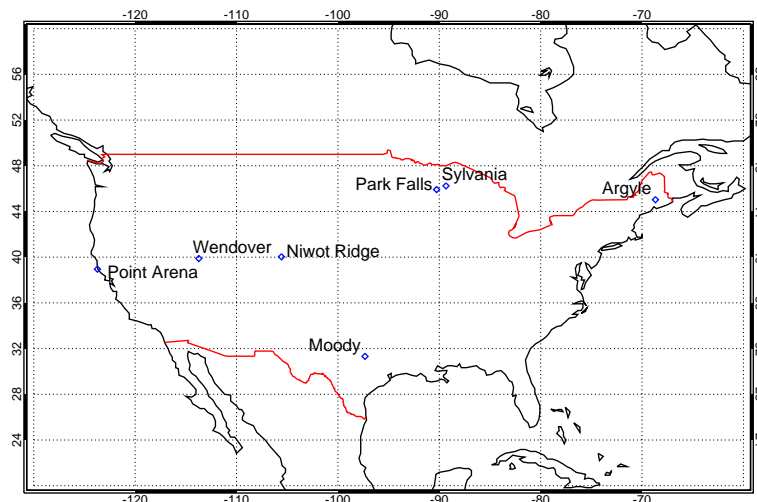


Fig. 11. The sampling locations over the USA for (a) surface sites: Niwot Ridge (40.03°N, 105.56° W, surface altitude = 3526 m), Point Arena (38.95° N, 123.72° W, 17 m) and Wendover (39.88° N, 113.717° W, 1320 m) and (b) tower sites: Argyle (45.03° N, 68.68° W, surface altitude = 157 m, maximum intake height = 107 m), Sylvania Tower (46.24° N, 89.34° W, 500 m, 36 m) and Moody Tower (31.32° N, 97.33° W, 256 m, 457 m). At Park Falls (45.92° N, 90.27° W, 868 m, 396.0 m) both surface and tower CO₂ measurements were available.

[Title Page](#)[Abstract](#)[Introduction](#)[Conclusions](#)[References](#)[Tables](#)[Figures](#)[◀](#)[▶](#)[◀](#)[▶](#)[Back](#)[Close](#)[Full Screen / Esc](#)[Printer-friendly Version](#)[Interactive Discussion](#)

EGU

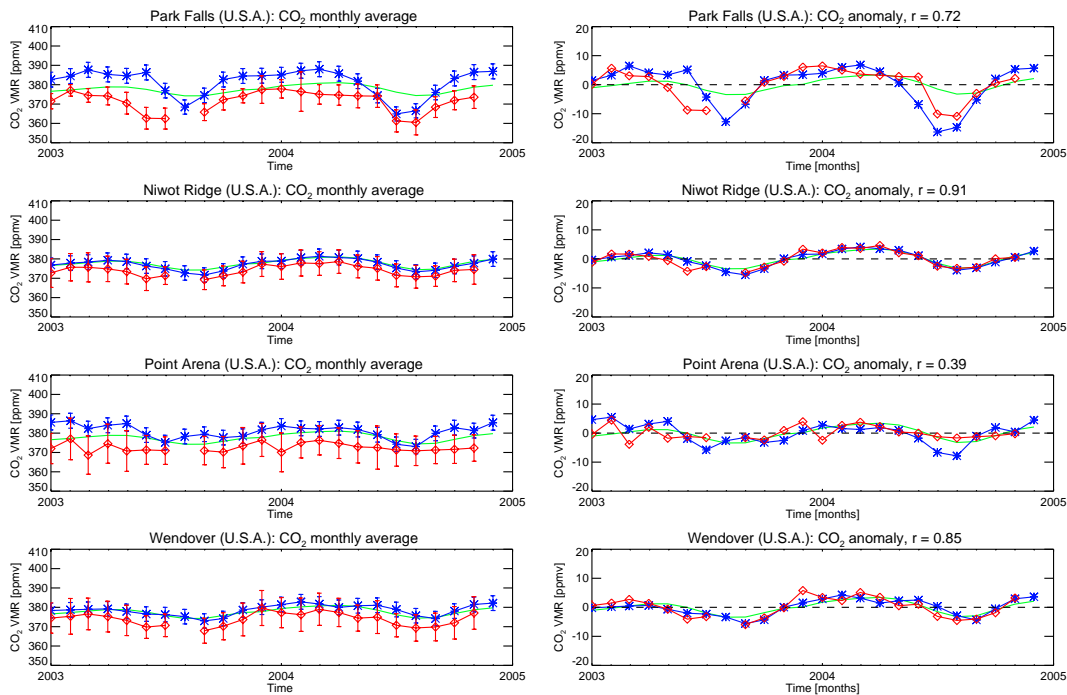


Fig. 12. As Fig. 9 but for the US surface in situ observations (blue) versus SCIAMACHY CO₂ (red) over the USA.

[Title Page](#)
[Abstract](#)
[Introduction](#)
[Conclusions](#)
[References](#)
[Tables](#)
[Figures](#)
[◀](#)
[▶](#)
[◀](#)
[▶](#)
[Back](#)
[Close](#)
[Full Screen / Esc](#)
[Printer-friendly Version](#)
[Interactive Discussion](#)

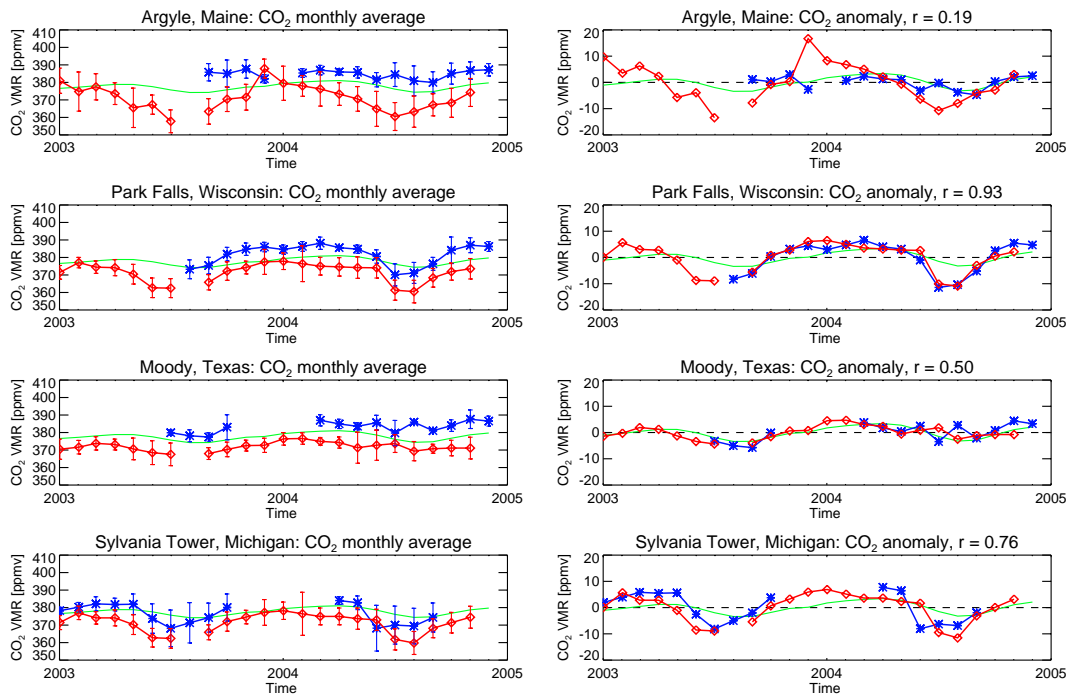


Fig. 13. As Fig. 9 but for the US tower observations (blue) versus SCIAMACHY CO₂ (red).

[Title Page](#)
[Abstract](#)
[Introduction](#)
[Conclusions](#)
[References](#)
[Tables](#)
[Figures](#)
[◀](#)
[▶](#)
[◀](#)
[▶](#)
[Back](#)
[Close](#)
[Full Screen / Esc](#)
[Printer-friendly Version](#)
[Interactive Discussion](#)

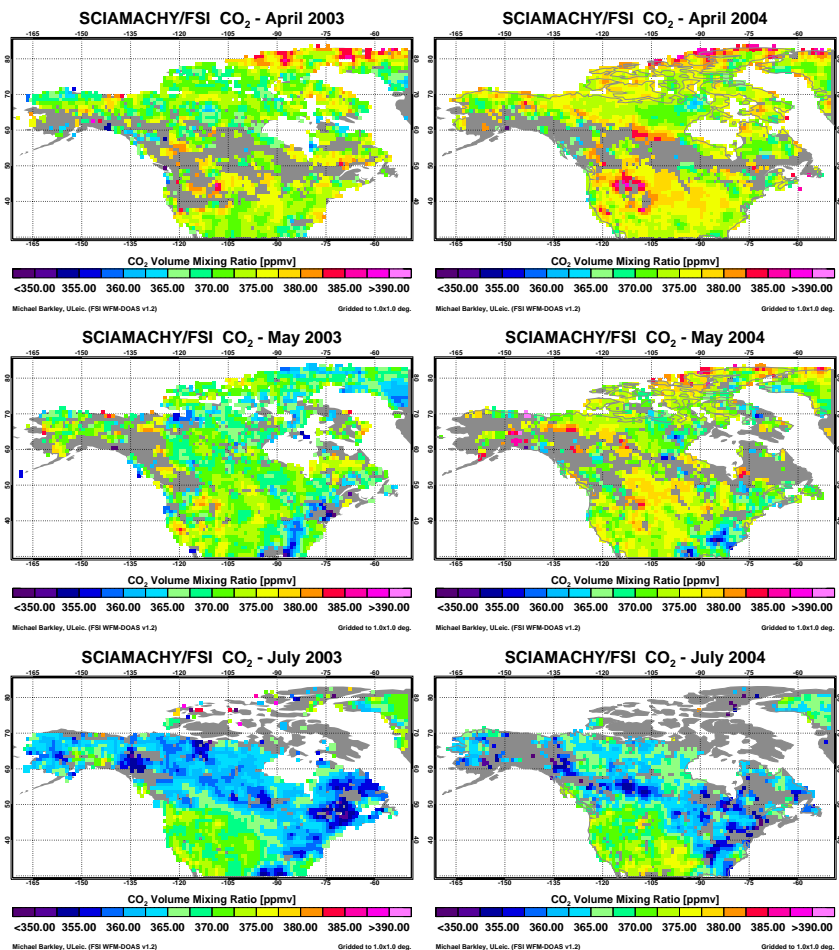


Fig. 14. SCIAMACHY observations over North America for April, May and July 2003 (left panels) and 2004 (right panels). All retrievals have been gridded to $1^\circ \times 1^\circ$ and smoothed with a $3^\circ \times 3^\circ$ box car average.

[Title Page](#)[Abstract](#)[Introduction](#)[Conclusions](#)[References](#)[Tables](#)[Figures](#)[◀](#)[▶](#)[◀](#)[▶](#)[Back](#)[Close](#)[Full Screen / Esc](#)[Printer-friendly Version](#)[Interactive Discussion](#)

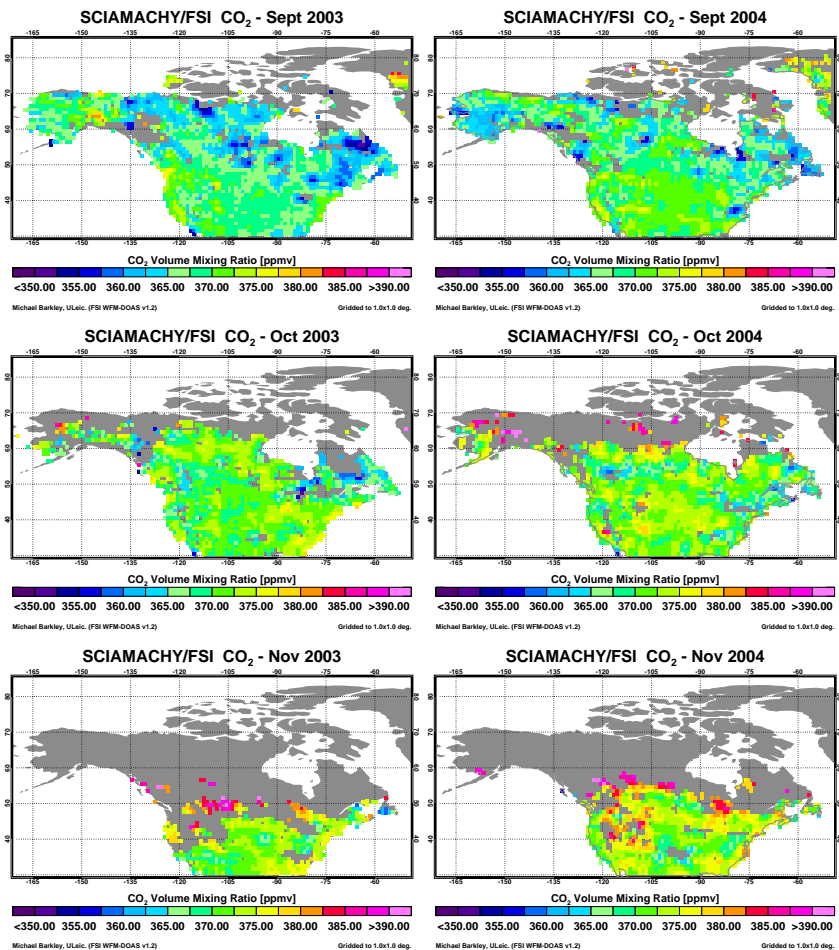


Fig. 15. As Fig. 14 but for September, October and November 2003–2004.

[Title Page](#)
[Abstract](#)
[Introduction](#)
[Conclusions](#)
[References](#)
[Tables](#)
[Figures](#)
[◀](#)
[▶](#)
[◀](#)
[▶](#)
[Back](#)
[Close](#)
[Full Screen / Esc](#)
[Printer-friendly Version](#)
[Interactive Discussion](#)

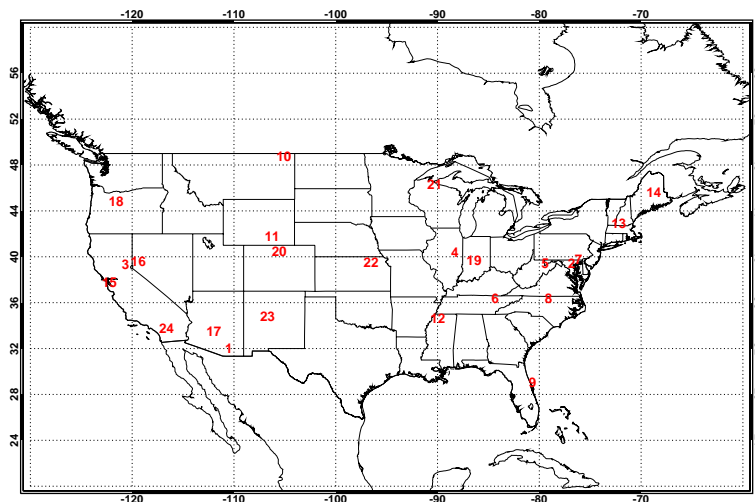
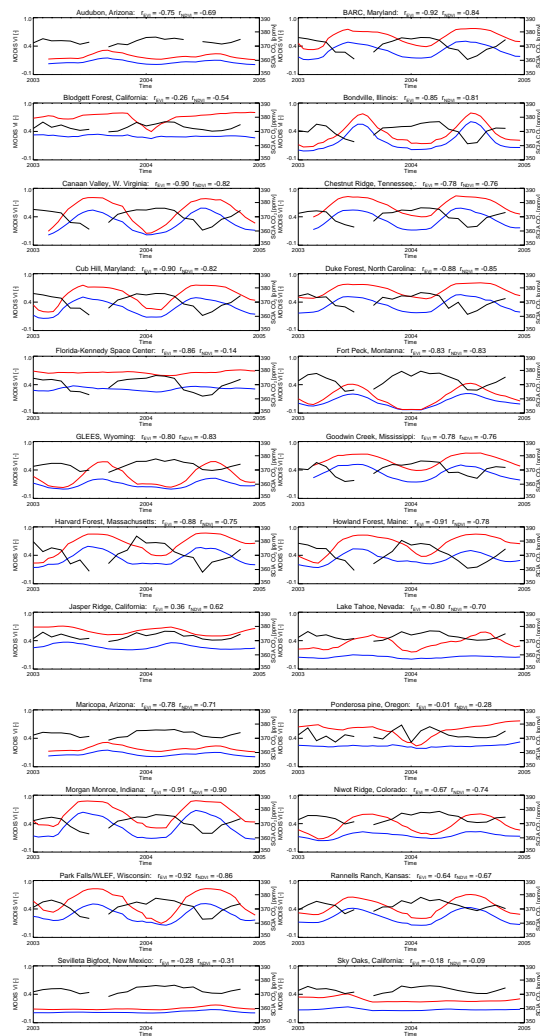


Fig. 16. The locations used in the SCIAMACHY/MODIS comparison (see Table 5): 1. Audubon Research Ranch, Arizona, 2. Beltsville Agricultural Research Center, Maryland, 3. Blodgett Forest, California, 4. Bondville, Illinois, 5. Canaan Valley, West Virginia, 6. Chestnut Ridge, Oak Ridge, Tennessee, 7. Cub Hill (Baltimore), Maryland, 8. Duke Forest - loblolly pine, North Carolina, 9. Florida-Kennedy Space Center (scrub oak), 10. Fort Peck, Montana, 11. GLEES, Wyoming, 12. Goodwin Creek, Mississippi, 13. Harvard Forest EMS Tower, Massachusetts, 14. Howland Forest (west tower), Maine, 15. Jasper Ridge, California, 16. Lake Tahoe, Nevada, 17. Maricopa Agricultural Center, Arizona, 18. Metolius-intermediate aged ponderosa pine, Oregon, 19. Morgan Monroe State Forest, Indiana, 20. Niwot Ridge Forest, Colorado, 21. Park Falls/WLEF, Wisconsin, 22. Rannells Ranch (ungrazed), Kansas, 23. Sevilleta BigFoot, New Mexico and 24. Sky Oaks, Young Stand, California.

[Title Page](#)
[Abstract](#)
[Introduction](#)
[Conclusions](#)
[References](#)
[Tables](#)
[Figures](#)
[◀](#)
[▶](#)
[◀](#)
[▶](#)
[Back](#)
[Close](#)
[Full Screen / Esc](#)
[Printer-friendly Version](#)
[Interactive Discussion](#)


[Title Page](#)
[Abstract](#)
[Introduction](#)
[Conclusions](#)
[References](#)
[Tables](#)
[Figures](#)
[Back](#)
[Close](#)
[Full Screen / Esc](#)
[Printer-friendly Version](#)
[Interactive Discussion](#)

**SCIAMACHY
atmospheric CO₂**

Barkley et al.

[Title Page](#)[Abstract](#)[Introduction](#)[Conclusions](#)[References](#)[Tables](#)[Figures](#)[I◀](#)[▶I](#)[◀](#)[▶](#)[Back](#)[Close](#)[Full Screen / Esc](#)[Printer-friendly Version](#)[Interactive Discussion](#)

Fig. 17. SCIAMACHY CO₂ (black line) plotted against MODIS NDVI (red line) and EVI (blue line) data, for selected sites within the U.S. for the time period 2003–2004. Both the NDVI and EVI data were scaled by 0.0001.

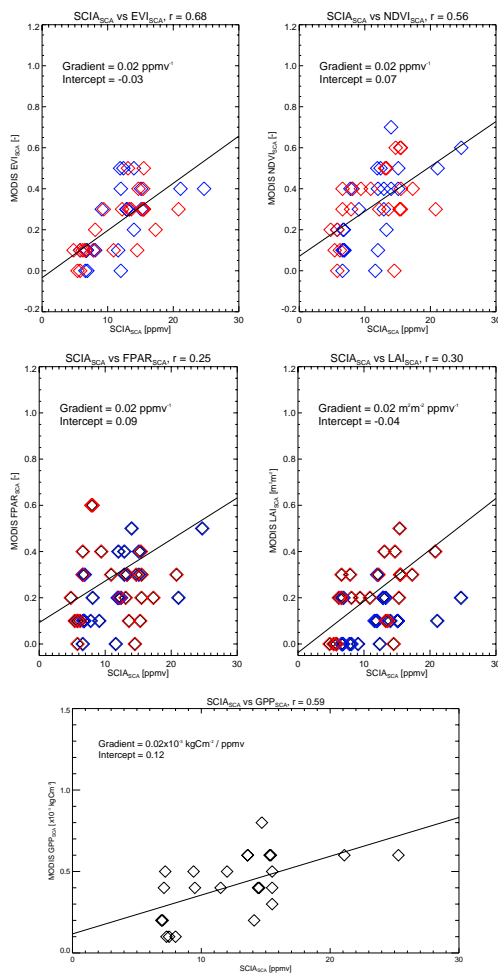


Fig. 18. Plots of the MODIS vegetation proxy seasonal cycle amplitudes against those of SCIAMACHY's CO₂ separated into the years 2003 (blue) and 2004 (red).

[Title Page](#)
[Abstract](#)
[Introduction](#)
[Conclusions](#)
[References](#)
[Tables](#)
[Figures](#)
[◀](#)
[▶](#)
[◀](#)
[▶](#)
[Back](#)
[Close](#)
[Full Screen / Esc](#)
[Printer-friendly Version](#)
[Interactive Discussion](#)